

# EFFECT OF GEOMETRIC NON - LINEARITY ON CRACKS IN PLATES SUBJECTED TO IMPACT LOADING - AN F.E. ANALYSIS

by

L. NAVEEN KUMAR

ME

1997

M

KUM

EFF



DEPARTMENT OF MECHANICAL ENGINEERING

INDIAN INSTITUTE OF TECHNOLOGY KANPUR

APRIL, 1997

**EFFECT OF GEOMETRIC NON-LINEARITY ON CRACKS IN PLATES  
SUBJECTED TO IMPACT LOADING - AN F. E. ANALYSIS**

**A Thesis Submitted**

**in Partial Fulfillment of the requirement**

**For the Degree of**

**MASTER OF TECHNOLOGY**

**by**

**L. NAVEEN KUMAR**

**to the**

**DEPARTMENT OF MECHANICAL ENGINEERING**

**INDIAN INSTITUTE OF TECHNOLOGY, KANPUR**

**APRIL, 1997**

- 9 MAY 1997

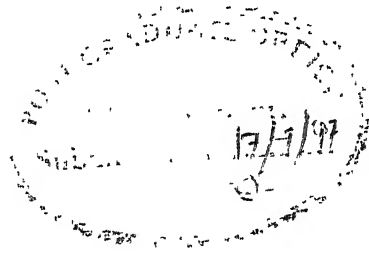
CENTRAL : CPARY

---

Case No. A 123346

## CERTIFICATE

This is to certify that the present work titled '**EFFECT OF GEOMETRIC NON-LINEARITY ON CRACKS IN PLATES SUBJECTED TO IMPACT LOADING - AN F.E.ANALYSIS**' by **Naveen Kumar** has been carried out under my supervision and has not been submitted elsewhere for the award of degree.



*NN Kishore*  
**Dr. N. N. KISHORE** 17/4

Professor

Mechanical Engg. Dept.

I. I. T. Kanpur

INDIA

April, 1997

## **ACKNOWLEDGEMENTS**

I express my deep sense of gratitude and indebtedness to Prof. N. N. Kishore for his invaluable guidance and constructive suggestions throughout the present work. He has been sympathetic and affectionate in moments of despair.

I am grateful to Atul Agarwal for his help in doing this work. It gives me immense pleasure to recall my association with Anand, Sunil, Reddy, Chalam, Rama Rao, Eswar, Murthy and all other friends who made my stay at IITK memorable.

April, 1997

**L.NAVEEN KUMAR**

# **CONTENTS**

**NOTATIONS**

**ABSTRACT**

<b>CHAPTER 1</b>	<b>INTRODUCTION</b>	<b>1</b>
1.1	Introduction	1
1.2	Literature Survey	3
1.3	Present work	7
<b>CHAPTER 2</b>	<b>BASIC EQUATIONS OF GEOMETRIC NON-LINEAR DYNAMIC PLATE ANALYSIS</b>	<b>9</b>
2.1	Governing Equations for Flexure of Thick Plate	9
2.2	Mixed Finite Element Formulation	12
2.3	Modification due to Geometric Non-Linearity	15
2.4	Finite Element Procedure for Inclusion of Geometric Non-Linearity	20
2.5	Iterative Scheme	25
<b>CHAPTER 3</b>	<b>IMPLEMENTATION OF FINITE ELEMENT CODE</b>	<b>30</b>
3.1	Element Selection	30
3.2	Time Integration Scheme	32

3.3	Newmark Implicit Scheme	33
3.4	Computer Implementation	35
CHAPTER 4	RESULTS AND DISCUSSION	37
4.1	Validation of the method	37
4.2	Effect of Geometric Non-Linearity in static case	38
4.3	Effect of Geometric Non-Linearity in Plate under Impact Loading	39
4.4	Geometric Non-Linearity on Crack in Plate on all Edges under Impact Loading	40
CHAPTER 5	CONCLUSIONS AND FUTURE WORK	48
5.1	Conclusions	48
5.2	Future Scope of Work	48
REFERENCES		49

## NOTATIONS

A	Part of elemental stiffness matrix
$a_0$ - $a_7$	Constants used in Newmark's Implicit Scheme
B	Part of elemental stiffness matrix
C	Part of elemental stiffness matrix
D	Part of elemental stiffness matrix
E	Modulus of elasticity
[F]	Part of elemental mass matrix
{f}	Load vector
G	Shear modulus of elasticity
h	Thickness of plate
L	Differential operator
$L_w$	Critical wave length
$L_e$	Effective length of an element
M	Mass matrix
N	Shape function
P	Part of elemental matrix
[K]	Stiffness matrix
q	Uniformly distributed load
S	Shear force
T	Edge moment
{U}	Displacement vector
u	Displacement in X-direction
v	Displacement in Y-direction



$w$	Displacement in Z-direction
$K_G$	Global stiffness matrix
$U_i$	Total displacements after $i^{\text{th}}$ load step
$\delta, \alpha$	Constants used in Newmark's Implicit scheme
$\epsilon$	Strain
$\Gamma$	Boundary
$\gamma$	Shear strain
$\nu$	Poisson's ratio
$\sigma$	Stress
$\theta$	Rotation
$\Omega$	Area
$\Delta t$	Time step
$K_\sigma$	Stiffness matrix due to stress level
$K_{nl}$	Non-Linear stiffness matrix
$K_T$	Total or tangential stiffness matrix
$dF$	Incremental applied load
$df_m$	The resultant load due to internal stress after $m$ equilibrium iterations
$\alpha$	Convergence limit

## **Abstract**

In practical cases when a plate is subjected to dynamic loading, the geometric and material linearity may not be preserved. This study is aimed at investigating the effect of geometric non-linearity in the dynamic response. As there are no closed form solutions available owing to the complexity of the problem, numerical methods are used to solve the problem.

For this computational work an efficient Finite Element code is developed using the “robust triangular element” developed by Zienkiewicz[1991]. “Mindlin plate theory” in the form of mixed formulation is used for modeling plate bending. Inertia effect of the element is represented by consistent mass matrix. When the displacements are finite the effect of geometric non-linearity is not small and it has to be taken into consideration. Due to geometric non-linearity the structure stiffens and it increases with displacement. Since the dynamic loading involves finite displacements, the effect of geometric non-linearity is analyzed in the present work.

The computer code is first used to solve a standard linear static problem and after its validation it was used to solve a standard problem considering geometric non-linearity, and then extended to solve the problem involving crack.

# CHAPTER 1

## INTRODUCTION

### 1.1 INTRODUCTION

In the analysis of many structural problems it is implicitly assumed that both displacements and strains developed are small. In practical terms it means that geometry of the elements remain basically unchanged during the loading process and first order infinitesimal linear strain approximations can be used. It also has the advantage of the behaviours of a plate under in-plane load and flexural load are independent of each other.

In practice such assumptions fail frequently even if strains may be small and elastic limits of ordinary structural materials are not exceeded. If accurate analysis is to be done and failure models are to be developed geometric non-linearity have to be considered in structures.

For instance stress due to membrane action usually neglected in plate flexure may cause considerable decrease of displacements as compared with linear solution even though displacements are still quite small. Further, when an in-plane compressive load reaches certain value, deflections increase more rapidly than predicted by linear solution and indeed a state may be attained where load carrying capacity decreases with continuing deformation.

The applications of such an analysis clearly is of considerable importance in aerospace applications, radio telescopes, cooling towers, and other relatively slender structures, and crack propagation in structures.

Many structures are subjected to dynamic loading. These loads may be created by moving vehicles, wind gusts, seismic disturbances, unbalanced machines, wave impacts, blasts. While solving these problems often the time variation is neglected and they are treated as static or quasi-static problems. However, if the time taken by the load to reach the maximum value is significantly less than fundamental period of the structure, then the inertia effect play an important role and the problem is termed as dynamic.

Geometric non-linearity effect is of significant value when displacements are large or strains are finite or both. Since many of dynamic loads are large giving rise to large displacements, geometric non-linearity has to be taken into consideration while solving such problems. The presence of cracks in plate structures subjected to suddenly applied loads like explosions makes study of dynamic fracture with geometric non-linearity necessary for developing sound design methodologies aimed at assuring the integrity of the structure and safety of the personnel. For many of the dynamic problems it is impossible to find out closed form solutions especially if they involve fracture. Thus, it often becomes mandatory to analyze dynamic crack propagation problems with geometric non-linearity, in finite solids using numerical methods.

## 1.2 LITERATURE SURVEY

The thin plate theory developed by Kirchhoff is modified for thick plates by Reissner and Mindlin by relaxing the assumption that the normals to the mid plane remain normal. This was done since the shear force terms cannot be neglected in many loading support conditions. Reissner and Mindlin theories can be extended to thick plates and thus known as Reissner-Mindlin formulation. Regarding Finite Element Method difference between thin plate and thick plate analysis is that in thick plate formulation instead of one approximate function for  $w$  (for calculation of rotational angle) three independent functions for deflection  $w$  and rotations  $\theta_x$ ,  $\theta_y$  are taken. In thin plates it is possible to represent the state of deformation by one quantity deflection  $w$  and thus its interpolation function is of a minimum  $C^1$  continuity is needed, while in the thick plates the interpolation functions for  $w$  along with rotation and shear degree of freedom need to be of  $C^0$  continuity.

While analytical solutions remain difficult for thick plates, the advent of Finite Element Method made thick plate theory simpler to implement. It is more convenient to start with thick plate formulation and can be used to thin plates if necessary, by imposition of certain relation between degrees of freedom [Zienkiewicz and Taylor,1991]. During formulation, if shear forces are eliminated, the formulation is known as irreducible formulation and if shear forces are retained it is known as hybrid formulation. The latter formulation gives more degree of freedom and so it is preferred in most of the cases [Zienkiewicz and Taylor,1991].

Other important factor is the selection of suitable element to perform satisfactorily for both thick and thin plates. While many elements are attempted to avoid problems of locking and singularity, the results by the use of 'robust triangular element' are found good [Zienkiewicz and Lefebvre,1988].

Generally in many structural problems it is assumed that both displacements and strains developed are small. This has the advantage of the behaviour of plate under in-plane and flexural loads independent of each other. The other important advantage is that the Finite Element analysis is far simpler and computationally faster as original configuration remains unchanged. In practice such assumptions fail frequently when strains are finite or deformations are large or both and elastic limits are not reached. For better designing 'Geometric non-linearity' should be considered. The application of geometric non-linearity has considerable importance in aerospace engineering, design of radio telescopes, cooling towers and many other [Zienkiewicz and Taylor ,1991].

In recent years a need has developed in industry to obtain non-linear analysis of structures subjected to static and dynamic loads. The earliest non-linear finite element analysis were essentially based on extensions of linear analysis and have been developed for specific applications [Oden,1972].

Closed form analytical solutions are available for only a limited range of structures and often involve gross simplifications. For most practical problems non-linear analysis can be carried out only by numerical techniques [Mondkar and

Basically two different approaches have been pursued in incremental non-linear finite element analysis. In the first static and kinematic variables are referred to updated configuration in each load step called as Eulerian or moving coordinate formulation. In second approach which is generally called Lagrangian formulation all static and kinematic variables are referred to initial configuration [Bathe, 1975].

On comparison of Eulerian and Lagrangian formulation for a simple truss structure a maximum difference of about 25 per cent in displacements was found [Yamada,1972]. It was found that Lagrangian formulation is more general and computational more efficient.

Of the various formulations of non-linearity some are general and some are restricted to account for material non-linearity only or for large displacements. Limited results have been obtained in dynamic non-linear analysis involving large displacements and finite strains. In dynamic analysis numerical time integration of finite element equations of motions is required .Extensive research is devoted towards the development of stable and accurate integration scheme. [Bathe, Ramm, Wilson,1975].

One of the important areas of concern is the iterative scheme to be used in non-linear problems. Physical insight into nature of the problem and usually small step incremental approaches are essential to obtain physically significant answers. In general, non-linear response will be computed by a combination of step by step and

iterative procedures. Depending on the degree of non-linearity equilibrium iterations may or may not be needed, and tangent stiffness may or may not be formulated in every step. Because of large computational effort typically required for decomposition of tangent stiffness matrix, it is desirable to seek a strategy in which the number of stiffness matrix reformulations are minimized [Modkar and Powell,1977].

Of the many iterative schemes to solve the non-linear problems Newton-Raphson method is found favourable in terms of ease in mathematical formulation, indeed it is the only process in which convergence is quadratic. [Simo and Taylor,1986]. The Newton-Raphson process despite its rapid convergence can be expensive and inconvenient since stiffness matrix has to be formed and factorized for each integration step. some times symmetric matrix becomes non symmetric. These drawbacks can be overcome by modified Newton-Raphson method, but this method suffers from a draw back of converging slowly [Zienkiewicz and Taylor,1991]. The convergence rate of modified Newton-Raphson method can be improved by selective relaxation iterative solution technique but this is highly problem-dependent. It will be very difficult to use this modification when both tension and compression are present [Carter Wellford and Halissen,1981].

It was only after the year 1960 that the stress problem of cracked plates are examined from a higher order plate bending theory taking shear deformation into account. The earliest attempt [Knowles, 1960] was concerned with the problem of infinite plate under uniform uniaxial bending far from the crack and was restricted to the case of vanishingly small plate thickness.



The predictions of classical theory [Williams, 1975] are known to be erroneous with respect to the angular distribution of stress around the crack tip. Results reported [Hartranft, 1968] show that the stress intensity factor varies very rapidly in the  $h/a$  range of 0.0 to 0.25. In paper [Murty, 1981] the finiteness of the plate was taken into account and the analysis here was based on differential approach. Shear deformation was taken into account through the use of Reissner theory. No restriction was put on the  $h/a$  ratio so that thickness effect could automatically be taken into account.

Numerical solutions based on the finite element method have been obtained for a number of elastodynamic crack growth problems in two dimensions. Nishioka and Atluri [1986] gave a very elaborate information on analysis of dynamic fracture using finite element method. The most common ways to deal with the crack-tip region are to simulate crack growth through gradual release of element nodal forces or imbedding a moving element in which the interpolation functions are determined by the continuum near tip fields at the crack-tip in the mesh, and energy path integral considerations.

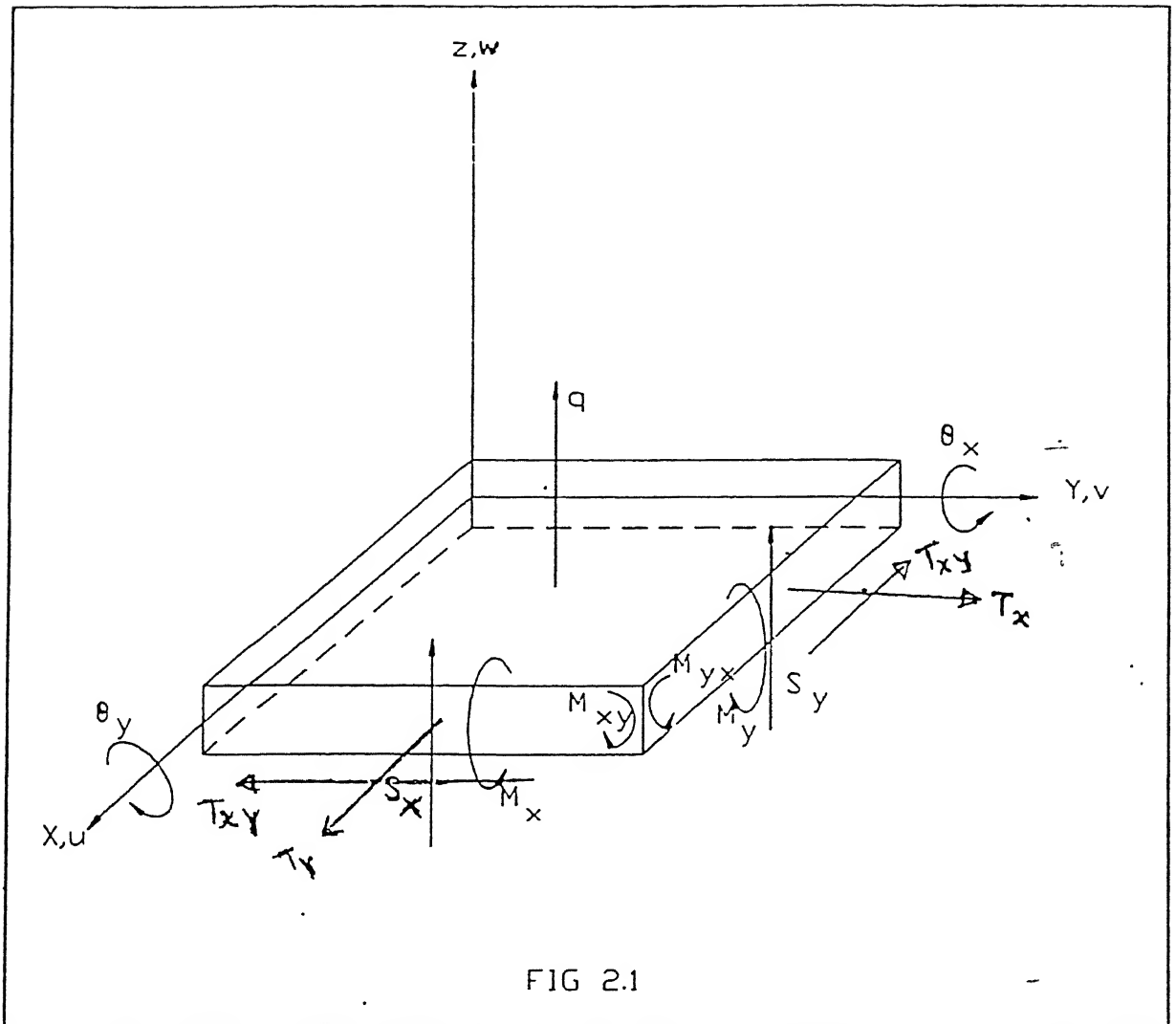
Research at the Defence Research Establishment, Suffield on vulnerability of naval structures has been directed to study the dynamic response of unstiffened and stiffened panels subjected to air blast shock waves. Numerical modelling using the finite element code ADINA has been contributed significantly to this research and has provided benchmark solutions. It involves a thin four noded shell element [Houlston and Slater, 1991] and use of isotropic elasto-plastic bilinear hardening material. The study highlights the importance of nonlinear analysis and the detailed approximations

to the actual boundary conditions.

A detailed analysis of the various time integration schemes from the point of view of accuracy and speed, were reported by [Seron et al., 1990; Zienkiewicz and Taylor, 1991; Bathe, 1990;]. It was concluded that, even though central difference scheme is the best in terms of computational speed and cost, Newmark's constant average scheme gives better accuracy and offers unconditional stability.

### **1.3 PRESENT WORK**

The present work deals with study of crack in plates when geometric non-linearity is considered under a static load and dynamic load (Suddenly applied load). A code developed by Dubey[1993] for linear plate analysis is taken as basis to further implement geometric non-linear analysis. The present work makes use of a mixed Finite Element Analysis using Reissner-Mindlin Plate theory is used to model the plate bending. To avoid locking or singularity a robust triangular element (T6/3 B3) [Zienkiewicz and Taylor, 1991] is used. Newmark's implicit scheme is used for time integration. Chapter 2 deals with theoretical part of the formulation of the plate bending, geometric non-linearity and the iterative scheme employed. Chapter 3 describes the Finite Element implementation of geometric non-linear analysis and integration with dynamics. Chapter 4 deals with the validation of the code and behaviour of plates under dynamic loading when geometric non-linearity is considered. Analysis of plate with crack under dynamic loading was also discussed. Chapter 5 deals with the conclusions of the present work and the scope of further work.



## CHAPTER 2

### BASIC EQUATIONS OF GEOMETRIC NON-LINEAR DYNAMIC PLATE ANALYSIS

This chapter presents the basic equations governing the thick plate under geometric non-linearity and dynamic conditions. Based on earlier chapter, a formulation based on Mindlin plate theory can be used for thick and thin plates.

#### 2.1 GOVERNING EQUATIONS FOR FLEXURE OF THICK PLATE

The Mindlin plate theory makes the following assumptions,

1. The strain and the stress components in Z-direction are negligible ( $\sigma_z$  and  $\epsilon_z \approx 0$ ) Fig. (2.1) where Z-direction represents the thickness direction.
2. The normals to the middle plane of the plate remains straight during deformation.

Applying above assumptions, equilibrium equations for plate bending problem can be obtained [Timoshenko, 1959] in terms of midplane rotations ( $\theta_x, \theta_y$ ), lateral displacements ( $w$ ) of the midplane and the shear forces ( $S_x, S_y$ ) at the cross-section. Sign convention and the variables are shown in Fig. (2.1).

Stress resultant moments and shear forces are defined in terms of stress variables as follows:

$$M_x = \int_{-h/2}^{h/2} \sigma_x Z dz , \quad M_y = \int_{-h/2}^{h/2} \sigma_y Z dz \quad (2.11 a)$$

$$M_{xy} = \int_{-h/2}^{h/2} \tau_{xy} Z dz \quad (2.11 b)$$

$$S_x = \int_{-h/2}^{h/2} \tau_{xy} dz , \quad S_y = \int_{-h/2}^{h/2} \tau_{yz} dz \quad (2.11 c)$$

For the dynamic analysis inertia forces due to mass and moment of inertia are considered in equilibrium equations. Formulating equilibrium equation using d'Alembert's principle, the following three equations are obtained.

$$\frac{\partial M_x}{\partial X} + \frac{\partial M_{xy}}{\partial Y} - S_x - \rho \frac{h^3}{12} \ddot{\theta}_x = 0 \quad (2.12a)$$

$$\frac{\partial M_{xy}}{\partial X} + \frac{\partial M_y}{\partial Y} - S_y - \rho \frac{h^3}{12} \ddot{\theta}_y = 0 \quad (2.12b)$$

$$\frac{\partial S_x}{\partial X} + \frac{\partial S_y}{\partial Y} + q - \rho h \ddot{w} = 0 \quad (2.12c)$$

where  $\ddot{\theta}_x, \ddot{\theta}_y, \ddot{w}$  represent acceleration of respective variables  $\theta_x, \theta_y, w$  and strain at a height of  $z$  from the centre plane are given as,

$$\epsilon_x = z \frac{\partial \theta_x}{\partial x}, \quad \epsilon_y = z \frac{\partial \theta_y}{\partial y} \quad (2.13a)$$

$$\gamma_{yz} = \theta_x + \frac{\partial w}{\partial x}, \quad \gamma_{xz} = \theta_y + \frac{\partial w}{\partial y} \quad (2.13b)$$

$$\gamma_{xz} = z \left[ \frac{\partial \theta_x}{\partial y} + \frac{\partial \theta_y}{\partial x} \right] \quad (2.13c)$$

## 2.2 THE MIXED FINITE ELEMENT FORMULATION

The finite element formulation involves expressing the three sets of variables  $\theta$ ,  $S$ ,  $w$ , at any point within the element in terms of nodal parameters of the element using shape functions.

$$\theta = \begin{bmatrix} \theta_x \\ \theta_y \end{bmatrix} = N_\theta \bar{\theta} \quad (2.14a)$$

$$S = \begin{bmatrix} S_x \\ S_y \end{bmatrix} = N_s \bar{S} \quad (2.14b)$$

$$w = N_w \bar{w} \quad (2.14c)$$

where  $\theta$ ,  $S$ ,  $w$  are the nodal values of respective variables.

Now using eqns. (2.13), (2.11) and eqn. (2.14) can be rewritten as follows:

$$\bar{\theta} - C_1 \bar{S} + \nabla \bar{w} = 0 \quad (2.15a)$$

$$L^T D L \bar{\theta} - \bar{S} - \rho \frac{h^3}{12} \bar{\theta} = 0 \quad (2.15b)$$

$$\nabla^T + Q - \rho h \bar{w} = 0 \quad (2.15c)$$

Where L,  $\nabla$  operators and  $C_1$  matrices are given by,

$$L = \begin{bmatrix} \frac{\partial}{\partial x} & 0 \\ 0 & \frac{\partial}{\partial y} \\ \frac{\partial}{\partial y} & \frac{\partial}{\partial x} \end{bmatrix}, \quad \nabla = \begin{bmatrix} \frac{\partial}{\partial x} \\ \frac{\partial}{\partial y} \end{bmatrix}, \quad C_1 = \frac{1}{Gh} \begin{bmatrix} 1 & 0 \\ 0 & 1 \end{bmatrix} \quad (2.16)$$

$$D = \frac{Eh^3}{12(1-\nu^2)} \begin{bmatrix} 1 & \nu & 0 \\ \nu & 1 & 0 \\ 0 & 0 & 0 \end{bmatrix} \quad (2.17)$$

Now by Galerkin method, using eqns. (2.14) and (2.15), and then integrating over the area of the element, the following equations are obtained:

$$A \bar{\theta} + B \bar{S} + E \bar{\theta} = \bar{F}_\theta \quad (2.18)$$

$$B^T \bar{\theta} - P \bar{S} + C \bar{w} = \bar{0} \quad (2.19)$$

$$C^T \bar{S} + F \bar{w} = \bar{F}_w \quad (2.20)$$

Where,

$$A = \int_{\Omega} (LN_{\theta})^T D (LN_{\theta}) d\Omega \quad , \quad B = \int_{\Omega} N_{\theta}^T N_s d\Omega$$

$$C = \int_{\Omega} N_s^T (\nabla N_w) d\Omega \quad P = \int_{\Omega} N_s^T C_1 N_s d\Omega$$

$$f_{\theta} = \int_{\Gamma_t} N_{\theta}^T d\Gamma, \quad f_w = \int_{\Omega} N_w^T q d\Omega$$

$$E = \frac{\rho h^3}{12} \int_{\Omega} N_{\theta}^T N_{\theta} d\Omega \quad , \quad F = \rho h \int_{\Omega} N_w^T N_w d\Omega$$

In the above equations the vector  $T$  represents two moment components imposed on the boundary by the traction and  $q$  is the intensity of the imposed lateral force. The shape functions  $N_{\theta}$ ,  $N_w$  are chosen to have  $C_0$  continuity, but because of shear forces are defined only for inside nodes of the element,  $N_s$  can be discontinuous between the elements. Such a choice allows  $S$  to be defined locally for each element and thus be eliminated when  $P$  is a non-singular matrix. Finally the problem includes only  $\theta$  and  $w$  as variables and the equilibrium equations can be expressed in terms of matrices as

$$\begin{bmatrix} A+BP^{-1}B^T & BP^{-1}C \\ C^TP^{-1}B^T & C^TP^{-1}C \end{bmatrix} \begin{bmatrix} \bar{\theta} \\ \bar{w} \end{bmatrix} + \begin{bmatrix} E & 0 \\ 0 & F \end{bmatrix} \begin{bmatrix} \ddot{\theta} \\ \ddot{w} \end{bmatrix} = \begin{bmatrix} f_{\theta} \\ f_w \end{bmatrix} \quad (2.21)$$



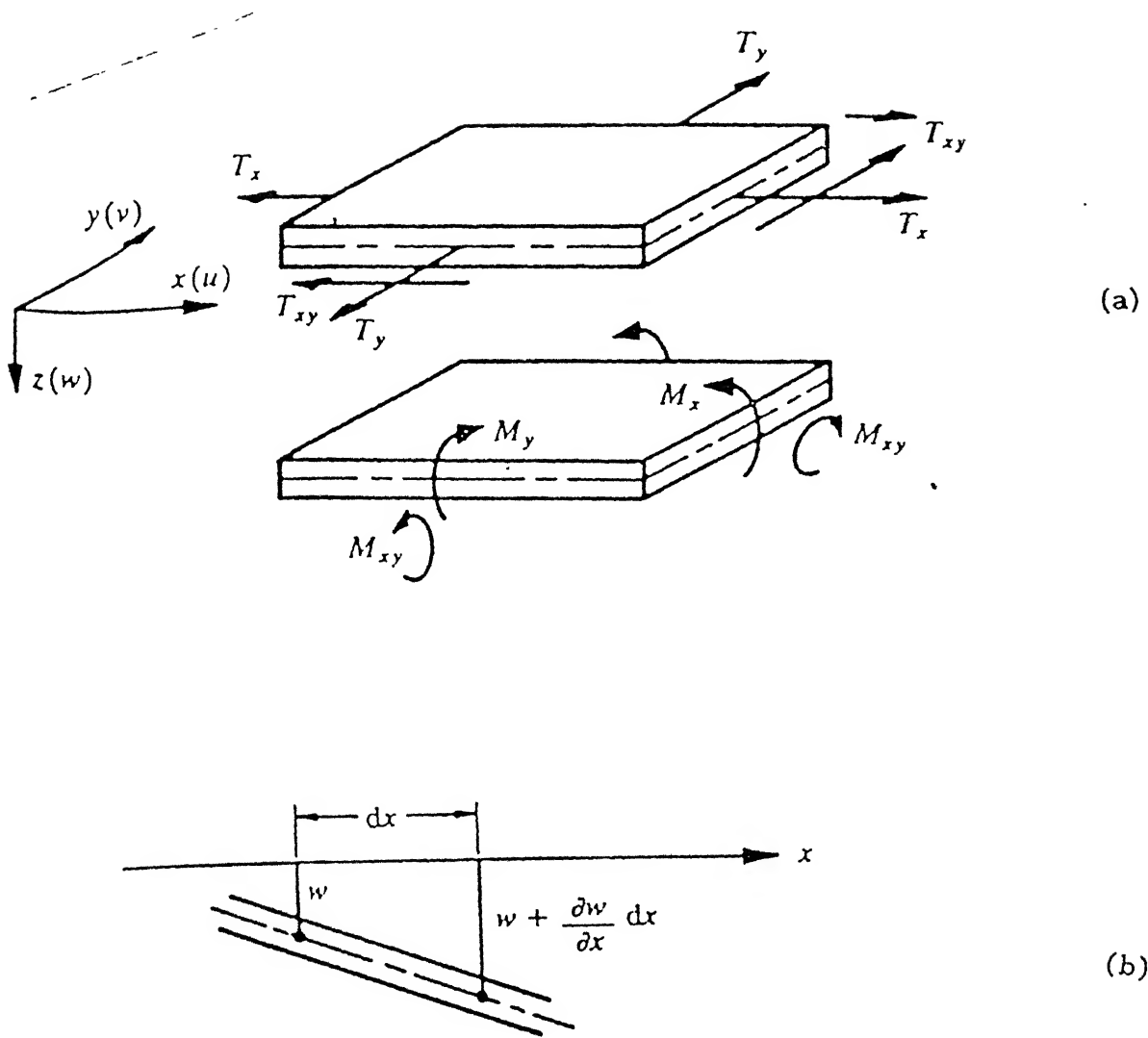


Fig 2.3 (a) In-plane and bending resultants for a flat plate.  
 (b) Increase of middle surface length due to lateral displacement.

In general eqn.(2.21) can be written as,

$$[K] \bullet [u] + [M] \bullet [\ddot{u}] = [F] \quad (2.22)$$

Where  $u$  consists of  $\theta_x, \theta_y, w$  nodal variables and  $[K]$  and  $[M]$  are the stiffness and mass matrices which can be obtained from equation (2.21).

### 2.3 MODIFICATION DUE TO GEOMETRIC NON-LINEARITY

A plate with  $u, v$  in-plane displacements in  $X$  and  $Y$  directions, and  $w$  is deflection in  $Z$  direction is subjected to in-plane and lateral forces is shown in Fig(2.3a). When the displacements are not very small the linear stress strain relations are not sufficient in predicting displacements or stresses. The in-plane and lateral deformations can not be dealt separately and they are coupled. The coupling is due to consideration of higher derivative terms.

From Fig(2.3b) it is seen that displacement  $w$  produces some additional extension in the  $x$  and  $y$  directions of the middle surface in addition to in-plane extensions  $u, v$  and the length  $dx$  stretches to

$$dx^1 = dx \sqrt{1 + \left(\frac{\partial w}{\partial x}\right)^2} \quad (2.23)$$

$$dx^1 = dx \left[ 1 + \frac{1}{2} \left(\frac{\partial w}{\partial x}\right)^2 - \frac{1}{8} \left(\frac{\partial w}{\partial x}\right)^4 + \dots \right] \quad (2.24)$$

where 'w' is lateral deflection of the plate,

'dx' is length of a strip when the lateral deflection is zero,

'dx<sup>1</sup>' is the elongated length of the strip after certain lateral deflection.

Including one higher order terms the total elongation in x direction can be written as

$$\epsilon_x = \frac{\partial u}{\partial x} + \frac{1}{2} \left( \frac{\partial w}{\partial x} \right)^2 \quad (2.25)$$

Where, 'u' displacement in X direction.

First term in the above equation (2.33) is due to in-plane loads, second term is due to lateral deflection. The second term in the above equation is taken to be negligible in case of small deflections. The second term in the above equation couples in-plane and lateral displacements.

In a similar way higher derivative terms are considered for other components. The plate strains are defined in terms of mid surface displacements and curvatures.

Strains and curvatures are written as

$$[ \epsilon ] = \begin{bmatrix} \epsilon_x \\ \epsilon_y \\ \gamma_{xy} \\ \kappa_x \\ \kappa_y \\ \kappa_{xy} \end{bmatrix} = \begin{bmatrix} \frac{\partial u}{\partial x} \\ \frac{\partial v}{\partial y} \\ \frac{\partial u}{\partial y} + \frac{\partial v}{\partial x} \\ -\frac{\partial^2 w}{\partial x^2} \\ -\frac{\partial^2 w}{\partial y^2} \\ 2 \frac{\partial^2 w}{\partial x \partial y} \end{bmatrix} + \begin{bmatrix} \frac{1}{2} \left( \frac{\partial w}{\partial x} \right)^2 \\ \frac{1}{2} \left( \frac{\partial w}{\partial y} \right)^2 \\ \left( \frac{\partial w}{\partial x} \right) \left( \frac{\partial w}{\partial y} \right) \\ 0 \\ 0 \\ 0 \end{bmatrix} \quad (2.26)$$

To be concise above equation can be written as

$$\epsilon = \begin{bmatrix} \epsilon_o^p \\ \epsilon_o^b \end{bmatrix} + \begin{bmatrix} \epsilon_{nl}^p \\ 0 \end{bmatrix} \quad (2.27)$$

Where superscript 'p' represents in-plane, 'b' represents bending and subscript 'nl' represents non-linear components

The in-plane stresses and moments resultants are represented in vector form as

$$[\sigma] = \begin{bmatrix} T_x \\ T_y \\ T_{xy} \\ M_x \\ M_y \\ M_{xy} \end{bmatrix} = \begin{bmatrix} \sigma^p \\ \sigma^b \end{bmatrix} \quad (2.28)$$

The 'stresses' are defined in terms of the usual resultants as

$$\begin{aligned} T_x &= \overline{\sigma_x} t \\ T_y &= \overline{\sigma_y} t \\ T_{xy} &= \overline{\tau_{xy}} t \end{aligned} \quad (2.29)$$

Where  $\overline{\sigma_x}$ ,  $\overline{\sigma_y}$ ,  $\overline{\tau_{xy}}$  are the average membrane stresses and, 't' is the thickness of the plate

Assuming material to behave linearly the stress resultants and strains can be related by stiffness matrix D, defined as

$$D = \begin{bmatrix} D^p & 0 \\ 0 & D^b \end{bmatrix} \quad (2.30)$$

Where the in-plane component of D is

$$D^p = \frac{E}{1-\nu^2} \begin{bmatrix} 1 & \nu & 0 \\ \nu & 1 & 0 \\ 0 & 0 & \frac{1-\nu}{2} \end{bmatrix} \quad (2.31)$$

and flexure component of D is

$$D^b = \frac{Et^3}{12(1-\nu^2)} \begin{bmatrix} 1 & \nu & 0 \\ \nu & 1 & 0 \\ 0 & 0 & \frac{1-\nu}{2} \end{bmatrix} \quad (2.32)$$

The displacements are related to nodal parameters by shape functions, as

$$\begin{bmatrix} u \\ v \\ \theta_x \\ \theta_y \\ w \end{bmatrix} = N a^e \quad (2.33)$$

Where  $N$  is shape function matrix which is composed of

$$N_i = \begin{bmatrix} N_i^p & 0 \\ 0 & N_i^b \end{bmatrix} \quad (2.34)$$

Where 'i' corresponds to particular node,

$N_i^p$  is in-plane shape function,

$N_i^b$  is bending shape function.

$$a_i = \begin{bmatrix} a_i^p \\ a_i^b \end{bmatrix} \quad (2.35)$$

Where  $a_i^p$  is nodal parameters of in-plane,

$a_i^b$  is nodal parameters of bending,

Which can be represented as

$$a_i = \begin{bmatrix} U_i \\ V_i \end{bmatrix}, \quad a_i^b = \begin{bmatrix} \theta_{x i} \\ \theta_{y i} \\ w_i \end{bmatrix} \quad (2.36)$$

$\theta_x, \theta_y$  are the rotations in x and y directions.

$w_i$  is lateral deflection.

## 2.4 FINITE ELEMENT PROCEDURE FOR INCLUSION OF GEOMETRIC NON-LINEARITY

The finite element procedure for non-linear analysis is based on the fact that the displacements are large and equilibrium conditions between internal and external 'forces' have to be satisfied

$$\psi(a) = \int_V \bar{B}^T \sigma dV - \bar{F} \quad (2.37)$$

$\psi$  sum of external and internal generalized forces

$B$  is defined from strain displacement definition as

$$de = \bar{B} da \quad (2.38)$$

$$\bar{B} = B_o + B_{nl}(a) \quad (2.39)$$

$B_o$  is due to small deflection theory (that is due to first term of equation (2.33),  $B_{nl}$  is due to geometric non-linearity effect (that is due to second term in equation (2.33) ).

Thus by taking appropriate variations with respect to  $a$  of equation (2.41) it can be written as

$$d\psi = \int_V d\bar{B} \sigma dV + \int_V \bar{B}^T d\sigma dV = K_T da \quad (2.40)$$

Stress is related to strain by relation

$$\sigma = D \epsilon, \quad d\sigma = D d\epsilon \quad (2.41)$$

By using above relations  $d\psi$  is written as

$$d\psi = \int dB_{nl}^T \sigma dV + \bar{K} da \quad (2.42)$$

Where

$$\bar{K} = \int \bar{B}^T D \bar{B} dv = K_o + K_{nl} \quad (2.44)$$

$K_o^p$  in-plane stiffness matrix

$K_o^b$  bending stiffness matrix

$$K_{nl} = \int_v (B_o^T D B_{nl} + B_{nl}^T D B_{nl} + B_{nl}^T D B_o) dv \quad (2.44)$$

$$\int_v dB^T \sigma dv = K_\sigma da \quad (2.45)$$

$$d\psi = (K_o + K_\sigma + K_{nl}) da = K_T da \quad (2.46)$$

$K_{nl}$  stiffness matrix due to geometric non-linearity.

$K_T$  is total are tangential stiffness matrix

$K_\sigma$  is stiffness matrix dependent on stress level.



The above procedure for calculating tangential stiffness matrix in geometric non linear problem can be put in the following algorithm.

(1) Evaluation of the linear small deformation matrix.

$$K_o = \begin{bmatrix} K_o^p & 0 \\ 0 & K_o^b \end{bmatrix} \quad (2.47)$$

$$K_o^p = \int_v B_o^{pT} D^p B_o^p dv \quad (2.48)$$

$K^p$  is in-plane stiffness matrix.

$K^b$  is bending stiffness matrix calculated from equation(2.28)

(2) Evaluation of higher order deformation stiffness matrix

$$K_{nl} = \int_v (B_o^T D B_{nl} + B_{nl}^T D B_o + B_{nl}^T D B_o) dv \quad (2.49)$$

$$\text{where } B_o = \begin{bmatrix} B_o^p & 0 \\ 0 & B_o^b \end{bmatrix} \quad B_{nl} = \begin{bmatrix} 0 & B_{nl}^b \\ 0 & 0 \end{bmatrix} \quad (2.50)$$

On substituting  $B_o$  and  $B_{nl}$  in above equation  $K_{nl}$  can be written as

$$K_{nl} = \int_v \begin{bmatrix} 0 & B_o^{pT} D^p B_{nl}^b \\ \text{sym.}, & B_{nl}^{bT} D^b B_{nl}^b \end{bmatrix} dv \quad (2.51)$$

$B_{nl}$  is due to higher order deformation .

(b) Evaluation of  $B_{nl}$

From the strain-displacement relations

$$\begin{aligned}\epsilon_x &= \epsilon_{linear} + \epsilon_{non-linear} = \frac{\partial u}{\partial x} + \frac{1}{2} \left( \frac{\partial w}{\partial x} \right)^2 \\ \epsilon_y &= \frac{\partial v}{\partial y} + \frac{1}{2} \left( \frac{\partial w}{\partial y} \right)^2 \\ \gamma_{xy} &= \frac{\partial u}{\partial y} + \frac{\partial v}{\partial x} + \frac{1}{2} \left( \frac{\partial w}{\partial x} \right) \left( \frac{\partial w}{\partial y} \right)\end{aligned}\tag{2.52}$$

non-linear term can be written as

$$\epsilon_{non-linear} = \epsilon_{nl}^p = \frac{1}{2} \begin{bmatrix} \theta_x & 0 \\ 0 & \theta_y \\ \theta_y & \theta_x \end{bmatrix} \begin{bmatrix} \theta_x \\ \theta_y \end{bmatrix} = \frac{1}{2} A \theta\tag{2.53}$$

Where for the sake of simplicity it is assumed that

$$\theta_x = \frac{\partial w}{\partial x}, \quad \theta_y = \frac{\partial w}{\partial y}\tag{2.54}$$

$$\theta = \begin{bmatrix} \theta_x \\ \theta_y \end{bmatrix} = G a^b\tag{2.55}$$

$$B_{nl}^b = AG\tag{2.56}$$

(c) Evaluation of  $B_o p$

$$B_o^p = \begin{bmatrix} \frac{\partial}{\partial x} & 0 \\ 0 & \frac{\partial}{\partial y} \\ \frac{\partial}{\partial y} & \frac{\partial}{\partial x} \end{bmatrix} \begin{bmatrix} N_1, & 0, & N_2, & 0, & \dots \\ 0, & N_1, & 0, & N_2, & \dots \end{bmatrix} \quad (2.57)$$

Where  $\{N_1, N_2 \dots\}$  are shape functions of  $\theta_x$  and  $\theta_y$  respectively.

(3) Evaluation of  $K_\sigma$

$K_\sigma$  is dependent on the stress level, which found from the following equation

$$K_\sigma = \int_v \begin{bmatrix} 0 & 0 \\ G^T & dA^T \end{bmatrix} \begin{bmatrix} T_x \\ T_y \\ T_{xy} \\ M_x \\ M_y \\ M_{xy} \end{bmatrix} dv \quad (2.58)$$

After some manipulation of the above equation it can be written as

$$K_\sigma = \int_v G^T \begin{bmatrix} T_x & T_{xy} \\ T_{xy} & T_y \end{bmatrix} G dv \quad (2.59)$$

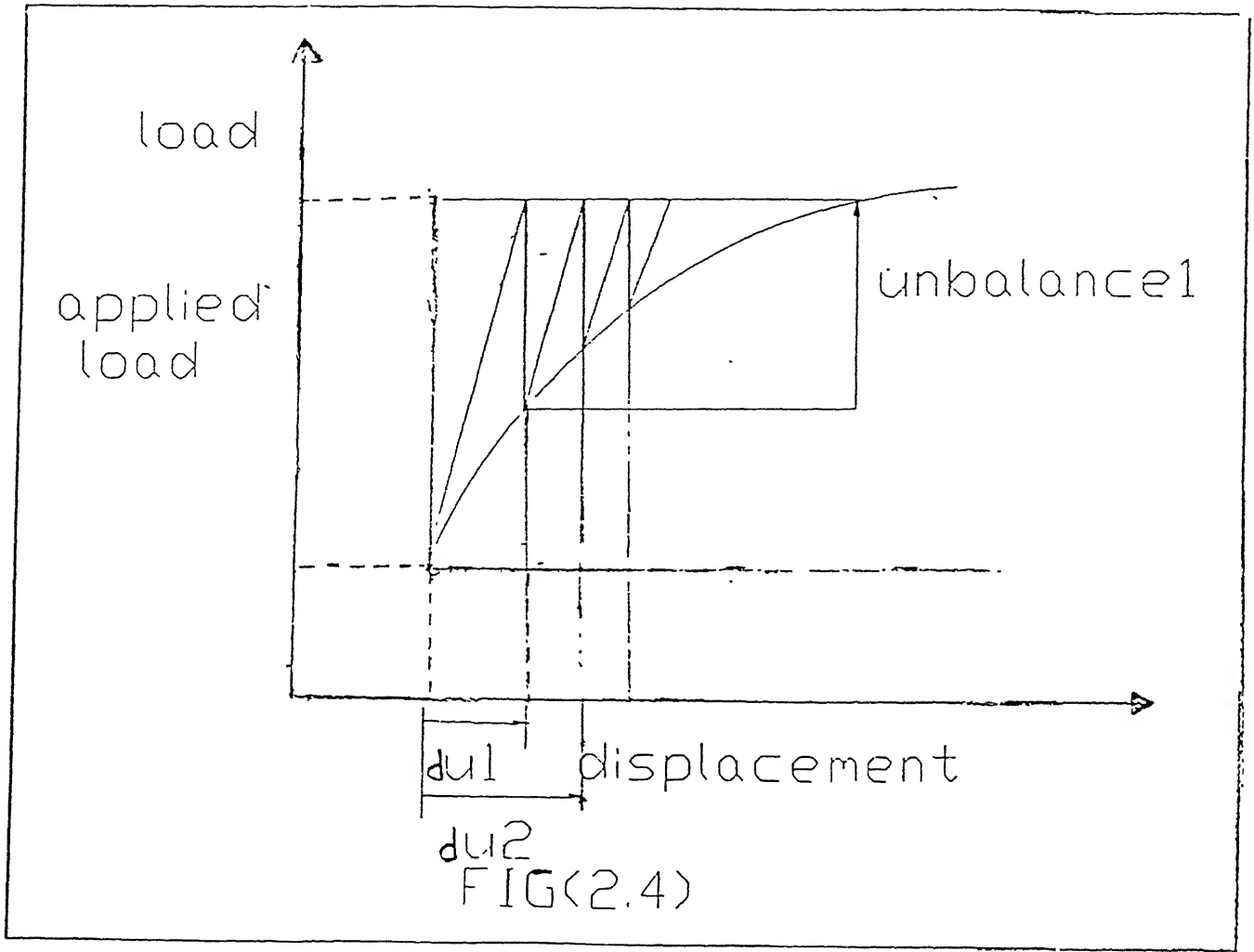
Where  $G$  is a shape function matrix of  $\theta_x$ , and  $\theta_y$  written as

$$G = \begin{bmatrix} N_1 & 0 & N_2 & 0 & N_3 & 0 & \dots \\ 0 & N_1 & 0 & N_2 & 0 & N_3 & \dots \end{bmatrix} \quad (2.60)$$

(4) Evaluation of tangential stiffness matrix

After evaluating in-plane and bending and stress dependent stiffness matrices, the total tangential stiffness matrix is calculated by this equation

$$K_T = K_o + K_\sigma + K_{nl} \quad (2.61)$$



This tangential stiffness matrix is used in finding non-linear displacements in plates. The next session deals with the iterative scheme used for getting non-linear displacements.

## 2.5 ITERATIVE SCHEME

Iterative scheme employs modified Newton Raphson method. In this method variable stiffness matrix is replaced by a constant stiffness matrix for a given load step. Even though convergence is slower in this method it reduces the computational time needed.

The basic equation for doing this iterative method

$$[U]_i = [U]_{i-1} + \sum_{m=1}^k dU_m \quad (2.62)$$

Left hand side of the eqn. (2.62) represents displacement after the  $i^{\text{th}}$  load step, and right hand side is sum of total displacement after  $(i-1)^{\text{th}}$  load step and displacement due to  $i^{\text{th}}$  load step.

$$K_G = f(U) \quad (2.63)$$

Where  $U$  represents displacement

$K_G$  represents global stiffness matrix.

$$dU_m = [K]_{i-1}^{-1} [dF - df_m] \quad (2.64)$$

$dF$  is the incremental applied load.

$df_m$  is the resultant load due to internal stresses after  $m$  equilibrium iterations.

$m$  is equilibrium iteration number.

The stiffness matrix used in the above equation is stiffness matrix corresponding to (i-1)<sup>th</sup> load step. But for calculating unbalanced loads it is required to calculate the stiffness matrix in each equilibrium iteration, which consumes considerable time. In order to reduce computational time unbalanced loads are calculated at elemental level and assembled.

The above eqn. (2.64) can be written as

$$df_m = [K_G]_{m-1} \sum_{j=1}^{m-1} du_j = \sum_{e=1}^n [K]_{m-1}^e \sum_{j=1}^{m-1} du_j \quad (2.54)$$

In the above eqn. (2.65), residual forces are calculated for every element and assembled. In the above equation  $[K_G]_{m-1}$  is updated stiffness matrix after (m-1) equilibrium iterations.

#### **convergence criterion :**

The error in each iteration is represented as follows,

$$e = [dU_m] - [dU_{m-1}]$$

Convergence is said to be achieved when

$$\frac{|e|}{|dU_m|} \leq \alpha$$

Where  $\alpha$  is predefined convergence limit.

## CHAPTER 3

### IMPLEMENTATION OF FINITE ELEMENT CODE

This chapter explains the different aspects of numerical method in developing the FEM code, including element selection.

#### 3.1 ELEMENT SELECTION

It is well known that complex geometric domains can be easily discretized into triangular elements. In literature for different types of problems, different types of elements are suggested as they should be free from defects of locking and singularity. The performance of the element under different type of loading and boundary conditions should also be stable. "Robust triangular element" with suitable nodal variables satisfy the stability conditions. [DUBEY,1993]

The choice of the shape functions and variables should be such that the Babushka-Brezzi[Zienkiewicz and Lefebvre,1988] conditions are satisfied by the system and thus, stability is ensured. The most vital and strictly necessary condition for the non-singularity of the system given by

$$\alpha = \frac{n_{\theta} + n_w}{n_s} \geq 1 \quad (3.1)$$

$$\beta = \frac{n_s}{n_w} \geq 1 \quad (3.2)$$

Where  $n_{\theta}$ ,  $n_s$ , and  $n_w$  stand for the number of variables for rotation, shear force and lateral displacements respectively in an element. If either of the two conditions are violated, the locking behaviour will occur in the solution.

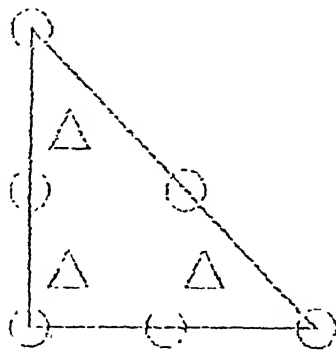
For the dynamic analysis if an implicit time integration scheme is used, it is necessary to use higher order finite elements and a consistent mass matrix. The higher order elements are effective in the representation of bending behaviour. These elements should be employed with consistent load vector, in that the mid side and corner nodes are subjected to their appropriate load contribution in the analysis.

In the mixed finite element formulation, triangular element (T6/3) has six boundary nodes which are used to determine a quadratic variation of  $\theta$  and  $w$  [Zienkiewicz and Lefebvre, 1988]. Shear forces are determined by a linear field by three internal nodes with no element inter connections fig(3.1a).

When standard patch tests [Zienkiewicz and Lefebvre, 1988; Zienkiewicz et al., 1986] are used with this element, the results indicate that, the element has incipient locking possibility and thus it is not a satisfactory element. But the examination of results indicate that the satisfaction of the requirements can be achieved by the addition of the  $\theta$  variables in the interior of the element. The three internal nodes created have the shape functions used of the form  $L_1^2 L_2 L_3$ , provide a new element (T6/3 B3) which passed the same patch test successfully in all cases [Zienkiewicz and Lefebvre, 1988], shown in fig(3.1b).

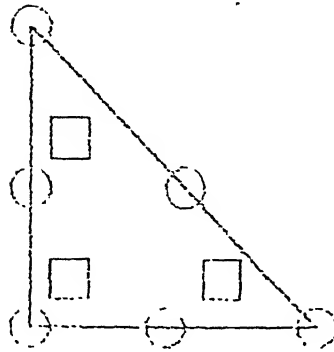
This particular element is chosen for the present analysis. It has 30 degree of freedom, and after the condensation of shear force terms the number of variables reduces to 24. And for consideration of in-plane displacement two degree of freedom are added to each of the 9 nodes, thus increasing total degree of freedom to 42, shown in the fig(3.1c)



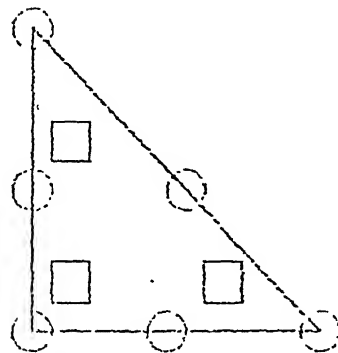


- $\bigcirc$   $\theta, w \cdot 2, 1, 1 \text{ dof}$   
 $\triangle$   $3 \cdot 2 \text{ dof}$   
 $\square$   $S, u \cdot 2, 2 \text{ dof}$

(a) T6/3 (21 degrees of freedom)



(b) T6/3 (30 degrees of freedom)



- $\bigcirc$   $\theta, w, u, v \cdot 2, 1, 1, 1 \text{ dof}$   
 $\square$   $S, \theta, u, v \cdot 2, 2, 1, 1 \text{ dof}$

(c) T6/3 (48 degrees of freedom)

Fig 3.1

### 3.2 TIME INTEGRATION SCHEME

The equation(2.29) is integrated by a numerical procedure. The integration is based on two ideas.

1. Static equilibrium including inertia force is achieved at discrete time intervals  $\Delta t$ .

$$[K]^{t+\Delta t} [u] + [M]^{t+\Delta t} [\ddot{u}] = [F]^{t+\Delta t} \quad (3.3)$$

2. Variation of displacement, velocity and acceleration within each time step is assumed. This assumption decides the accuracy and stability of the solution procedure.

The idea no 2 decides the time integration scheme. The choice of a scheme depends on the finite element idealisation. However, the finite element idealisation to be chosen depends in turn on the actual wave velocity of the medium to be analyzed. It follows, therefore the selection of an appropriate finite element idealization of a problem and the choice of effective integration scheme for the response solution are closely related and must be considered together.

Out of many schemes 'Newmark's implicit scheme is most accurate and unconditionally stable.

### 3.3 NEWMARK IMPLICIT SCHEME

The Newmark's constant acceleration scheme is written as follows [Bathe,1990],

$$\dot{U}^{t+\Delta t} = \dot{U}^t + [ (1 - \delta) \ddot{U}^t + \delta \ddot{U}^{t+\Delta t} ] \Delta t \quad (3.4a)$$

$$U^{t+\Delta t} = U^t + \dot{U}^t t + [ (\frac{1}{2} - \alpha) \ddot{U}^t + \alpha \ddot{U}^{t+\Delta t} ] \Delta t^2 \quad (3.5b)$$

Where  $\alpha$  and  $\delta$  are parameters that control integration accuracy and stability. Newmark originally proposed an unconditional stable scheme, in which case  $\delta = 0.5$  and  $\alpha = 0.25$ . Using eqn(3.3) and eqn(3.5) final form can be obtained as,

$$[K + a_0 M] U^{t+\Delta t} = F^{t+\Delta t} + [M] (a_0 U^t + a_2 \dot{U}^t + a_3 \ddot{U}^t) \quad (3.6a)$$

$$\ddot{U}^{t+\Delta t} = a_0 (U^{t+\Delta t} - U^t) - a_2 \dot{U}^t - a_3 \ddot{U}^t \quad (3.6b)$$

$$\dot{U}^{t+\Delta t} = \dot{U}^t + a_6 \ddot{U}^t + a_7 \ddot{U}^{t+\Delta t} \quad (3.6c)$$

$$\begin{aligned} a_0 &= \frac{4}{\Delta t^2} , & a_2 &= \frac{4}{\Delta t} , & a_3 &= 1 \\ a_6 &= \frac{\Delta t}{2} , & a_7 &= \frac{\Delta t}{2} \end{aligned} \quad (3.7)$$

The implicit scheme, as can be seen from the final formulation requires inversion of  $[K + a_0 M]$  matrix. For this purpose Cholesky decomposition technique is computationally efficient.

### 3.31 Time step

After deciding on time integration scheme, it is necessary to use a time step suitable with finite element mesh. If the critical wavelength in the medium is denoted by  $L_w$ , then the time step can be decided as ,

$$\Delta t = \frac{L_w}{c \cdot n}$$

And the effective length of a finite element should be

$$L_e = c \Delta t$$

Where 'c' is wave speed and 'n' is the number of nodes per critical wave length. The effective wave length and corresponding time step must be able to represent the complete bending wave accurately and is chosen appropriately depending on the kind of element idealization and time integration scheme used. It is reported that at least 8 nodes per shortest wave length are required in order to produce all artifacts of wave propagation [Seron, 1990]

However, for higher order (parabolic and cubic) continuum elements the time step has to be further reduced, because the interior nodes are stiffer than the corner nodes [bathe, 1990].

### **3.4 COMPUTER IMPLEMENTATION**

The computer code developed by Dindore[1994] has been enhanced to take into consideration of geometric non-linearity in the present work. Since geometric non-linearity is considered, load applied on plate should be in small increments and for each increment of load, convergence criteria has to be checked. In dynamic loading the time step used should be smaller when geometric non-linearity is considered than without, since the structure stiffens with the displacements.

In case of crack in plate under impact loading, it is assumed that an initial crack is present and it is extended and restored at every time step. Energy before crack extension and after crack extension is calculated, the difference of these two energies is the energy release.

Energy in plate is calculated by the expression,

$$P.E = \frac{1}{2} [u]^T [K] [u] + \frac{1}{2} [\dot{u}]^T [M] [\dot{u}] - [p] [u]^T \quad (3.8)$$

Where  $[u]$  is velocity vector,  $P$  is load vector,  $[K]$  is the stiffness matrix,  $[M]$  is the mass matrix.

## CHAPTER 4

### RESULTS AND DISCUSSIONS

This chapter is divided into two parts, first consists of validation of the present method while second part analyses the effect of geometric non-linearity in plate, with and without crack.

#### 4.1 VALIDATION OF THE METHOD

Validation of the present method is done in following cases.

Case 1: Stresses and deflections for a elastic problem are calculated for standard cases (Timoshenko, 1959). A problem of fixed plate subjected to concentrated load is considered (fig 4.1).

The material and geometric properties are as follows:

Modulus of elasticity,  $E = 200 \text{ Gpa}$

Poisson's ratio,  $\nu = 0.25$

Density,  $\rho = 7800 \text{ Kg/m}^3$

Thickness of the plate,  $h = 0.02 \text{ m}$

Length of the plate,  $L = 2 \text{ m}$

Considering the symmetry of the problem, only one quarter of the plate is analyzed. Mesh used is shown in the Fig 4.2. The mesh used is generated and optimized by an interactive preprocessor already developed (Kishore, 1996). An enlarged view showing details of the quarter plate is shown in Fig 4.3. Compared to the theoretical value of central deflection of 1.52cm for a load of 0.1MN, the F.E.M result obtained is 1.50cm. As can be seen, the value obtained by F.E.M is within 1.5% of the theoretical

value and is reasonably accurate.

Case 2: Deflections are calculated by considering geometric non-linearity effect for a standard case of rectangular plate fixed on all sides and subjected to uniform load. In this problem mesh used is same as that of in fig(4.2) and the material properties used as in case 1. Fig 4.4a shows the theoretical results given in Timoshenko and Krieger[1989]. Fig 4.4b shows the results obtained by the present method. Compared with the theoretical value of the central deflection,  $W_{\max}/h$ , of 1.52 the F.E.M results obtained a value of 1.49 for the same load value,  $qb^4/Dh$ , of 150. As can be seen the error of the present method is below 2%.

Case 3: The response of an elastic cantilever under dynamic condition was determined by the present method and compared with those given by Bathe and Ramm [1975] for the purpose of validation.

The material and geometric properties used are as follows:

Modulus of elasticity,  $E = 8.277 \text{ Mpa}$

Poisson's ratio,  $\nu = 0.2$

Density,  $\rho = 10.7 \text{ Kg/m}^3$

Thickness of the plate,  $h = 0.025 \text{ m}$

Length of the plate,  $L = 0.25 \text{ m}$

Uniformly distributed load,  $q_0 = 20292 \text{ N/m}^2$

The load is a suddenly applied step load shown in Fig 4.5a.

The variation of dynamic load is assumed as follows.

For load #1,

$$\begin{aligned} q &= 0.0 & \text{at} & t = 0 \\ q &= q_0 & \text{at} & t \geq 0 \end{aligned} \quad (4.1)$$

This loading as shown in fig(4.5a)

For load #2

$$\begin{aligned} q &= \frac{q_0}{2} \left[ 1 - \cos\left(\frac{\pi t}{RT}\right) \right] & t \leq RT \\ q &= q_0 & t > RT \end{aligned} \quad (4.2)$$

where RT is the rising time.

Mesh used is same as in Fig 4.3.

The element size and the time steps are chosen in such a way so that the solution remains stable. Time step was selected as a fraction of fundamental time period. In this, time step is taken as 45μs. As explained in earlier chapter the results were obtained using Newmark integration scheme.

Fig(4.6) presents the end deflection of the cantilever. For the present method gives maximum deflection,  $W_{\max}/L$ , of 0.76 which compares well with the value of 0.745 obtained by Bathe and Ramm [1975].

### 4.3 EFFECT OF GEOMETRIC NON-LINEARITY IN PLATE UNDER IMPACT LOADING

Fig 4.7 presents the end deflection of a cantilever subjected to impact loading



load #1 shown in Fig. 4.5a with geometric non-linearity. The figure also shows the results obtained for a plate without geometric non-linearity. As expected, it is seen in this figure that the cantilever stiffens with increasing displacements and there is decrease in amplitude and effective period of vibration.

When higher impact are loads applied the effect of geometric non-linearity is increased as seen in figures (4.7b) and (4.7c).

#### **4.4 GEOMETRIC NON-LINEARITY EFFECT ON CRACK IN PLATE UNDER IMPACT LOADING**

Fixed plate with a crack subjected to uniformly distributed impact load is shown in Fig 4.12. The plate is analyzed for two load cases:

Case 1: In this impact load #2 as shown in Fig 4.5b was applied. In this problem it was assumed that an initial central crack of length 71.4cm of the edge length was assumed. Time step of  $10\mu\text{s}$  was chosen. Mesh used was same as in Fig 4.2.

The material and geometric properties are as follows:

Modulus of elasticity,  $E = 200 \text{ Gpa}$

Poisson's ratio,  $\nu = 0.25$

Density,  $\rho = 7800 \text{ Kg/m}^3$

Thickness of the plate,  $h = 0.02 \text{ m}$

Length of the plate,  $L = 2 \text{ m}$

Fig 4.9 gives the variation of energy release rate as a function of time. It was observed that energy release rate is higher with geometric non-linear consideration than without geometric non linear consideration by 10.7 percent. This is due to the contribution of energy due to membrane stresses. These membrane stresses are

neglected in linear problem.

Case 2: For the same material properties, mesh and crack conditions as above and an impact load given by load #1 (Fig 4.5) the plate was analyzed. Fig 4.10 shows the variation of energy release rate as a function of time. It is observed in that energy release rate in both linear and non-linear case is high due to than case(1), in linear case it is by 5% in non-linear case it was by 10%. This is due to the extra energy that has been put in due to sudden initial rise of the applied load. The energy release to is higher with geometric non-linear consideration than without geometric non-linear consideration by nearly 18 percent.

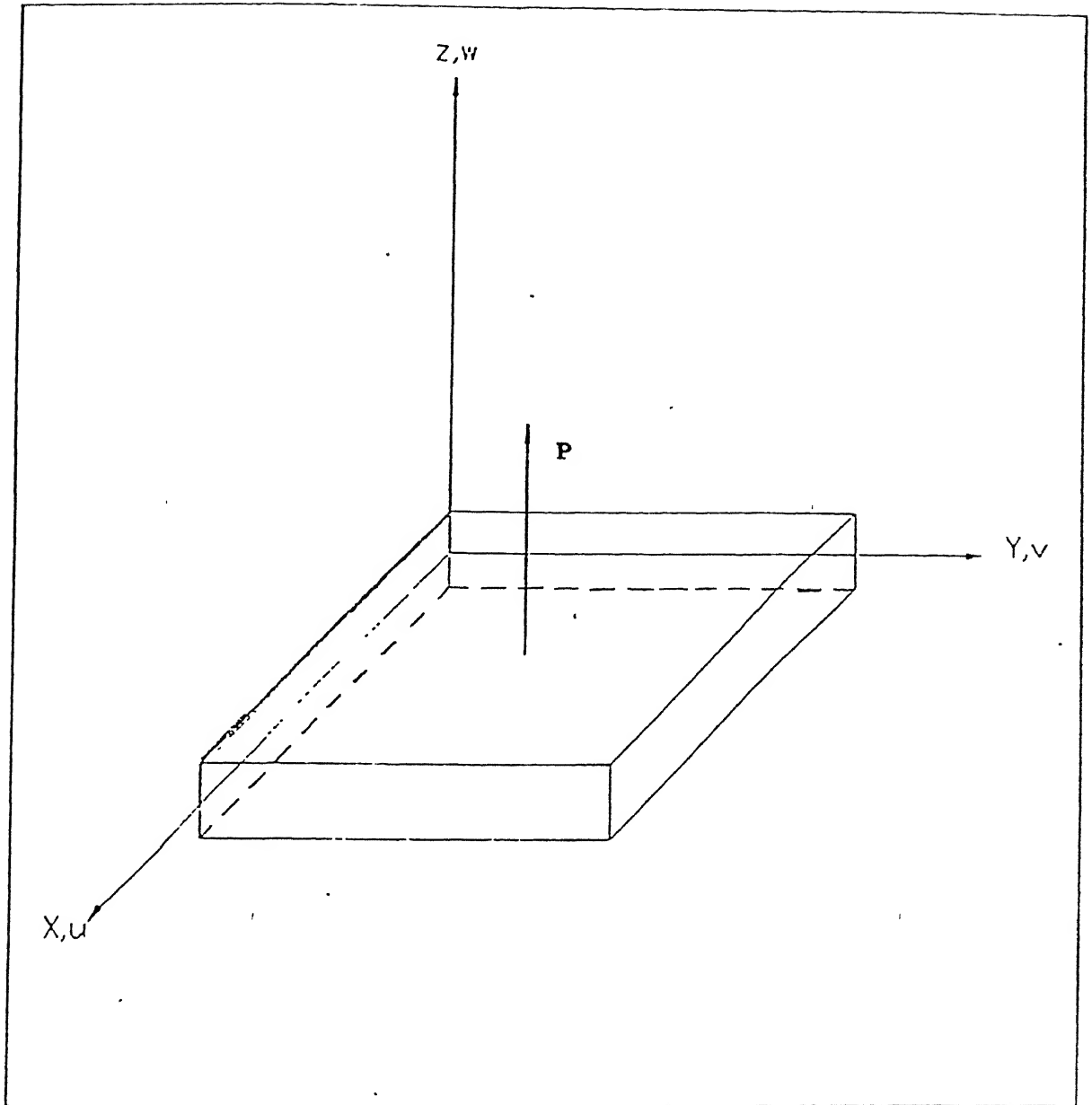


Figure 4.1. Plate subjected to a concentrated load  $p$  at the center.

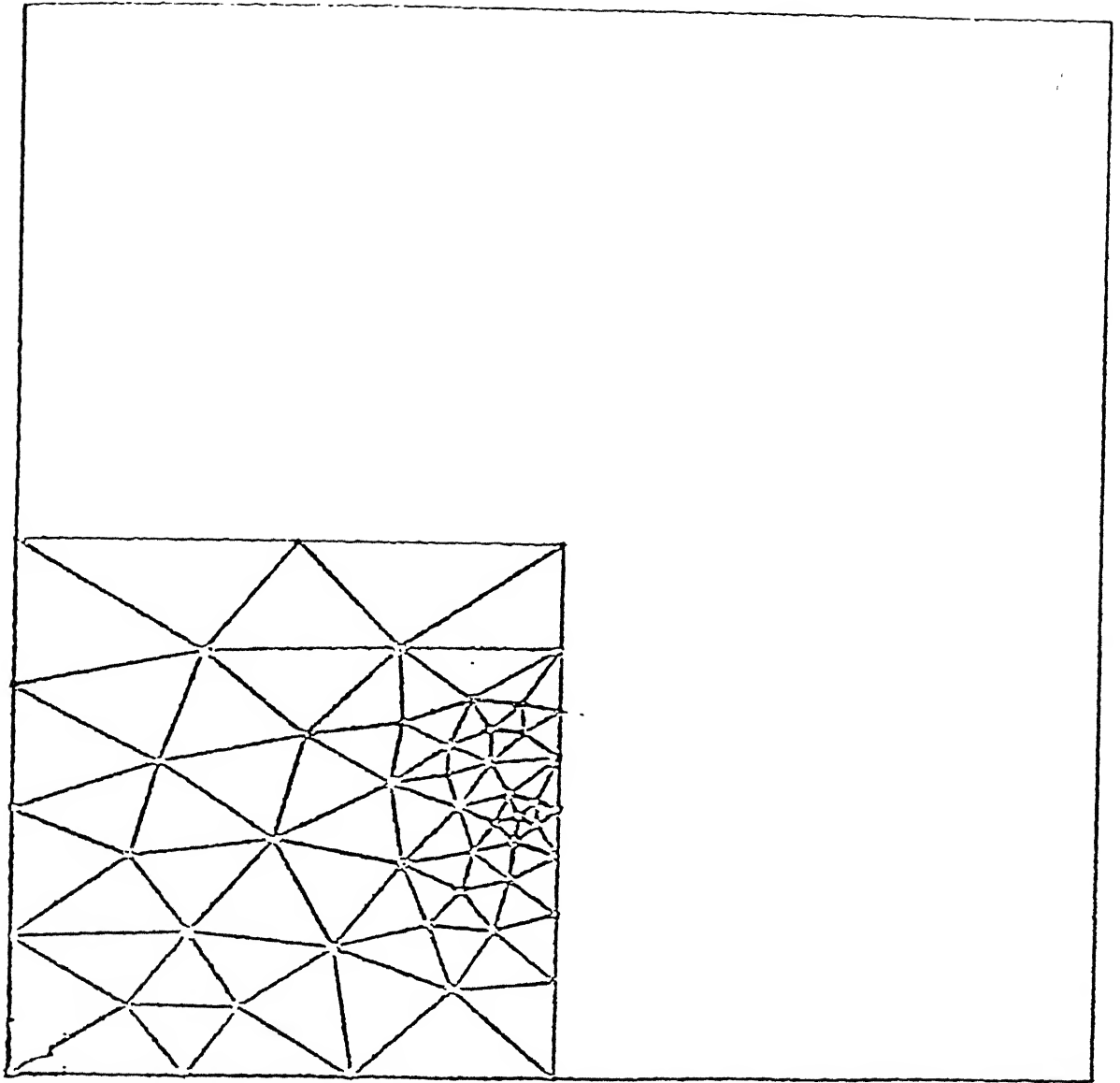


Figure 4.2. Mesh of 81 elements on the quarter portion of plate.

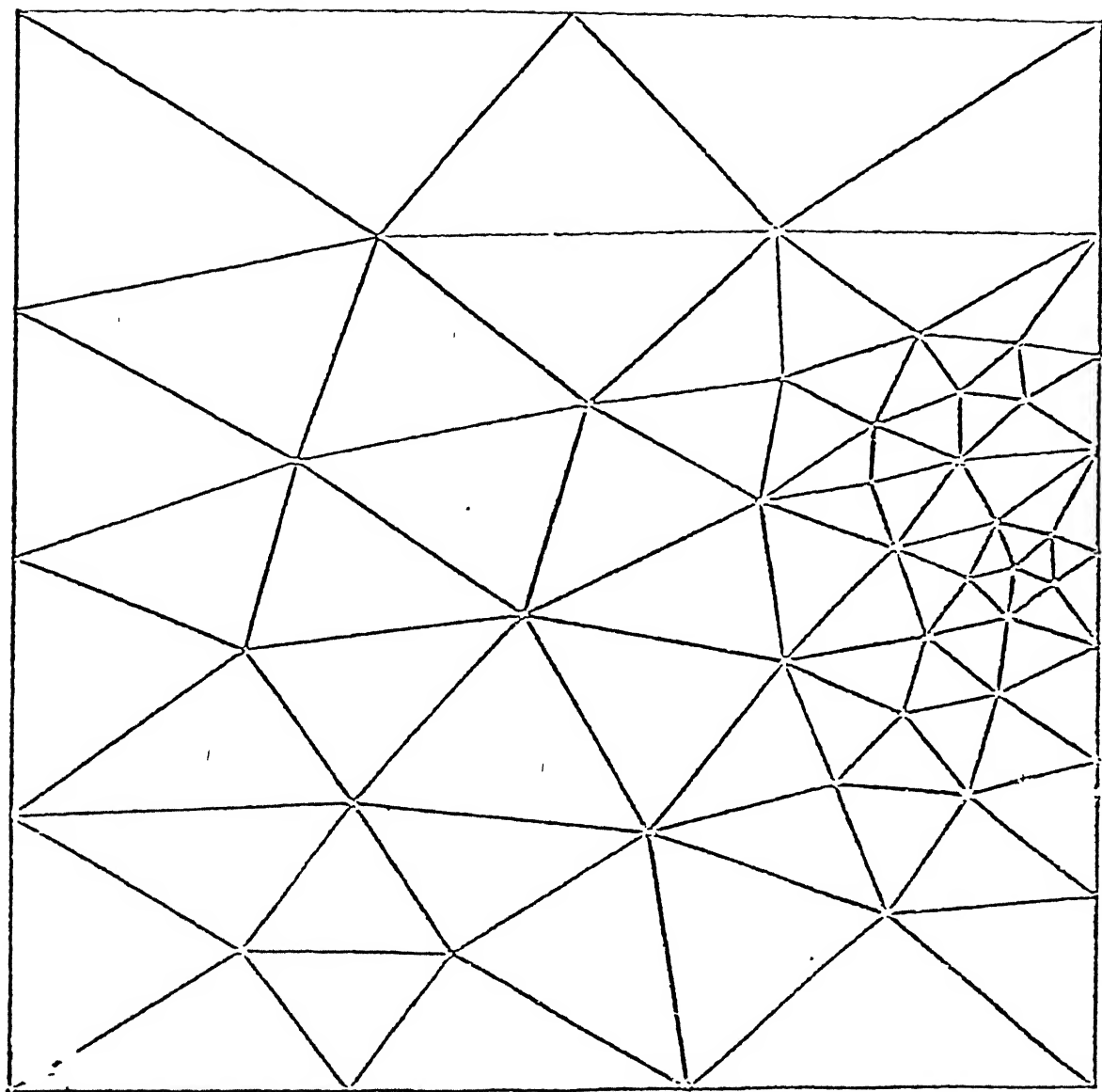


Figure 4.3. Enlarged quarter portion of the plate.

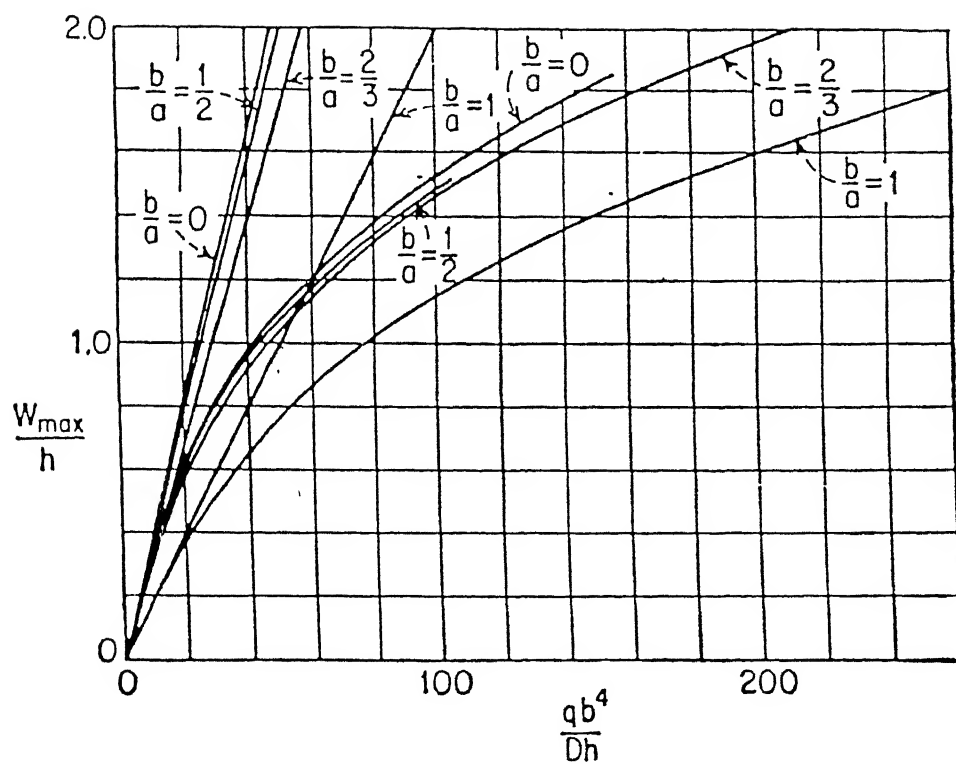


Fig 4.4(a) Theoretical results

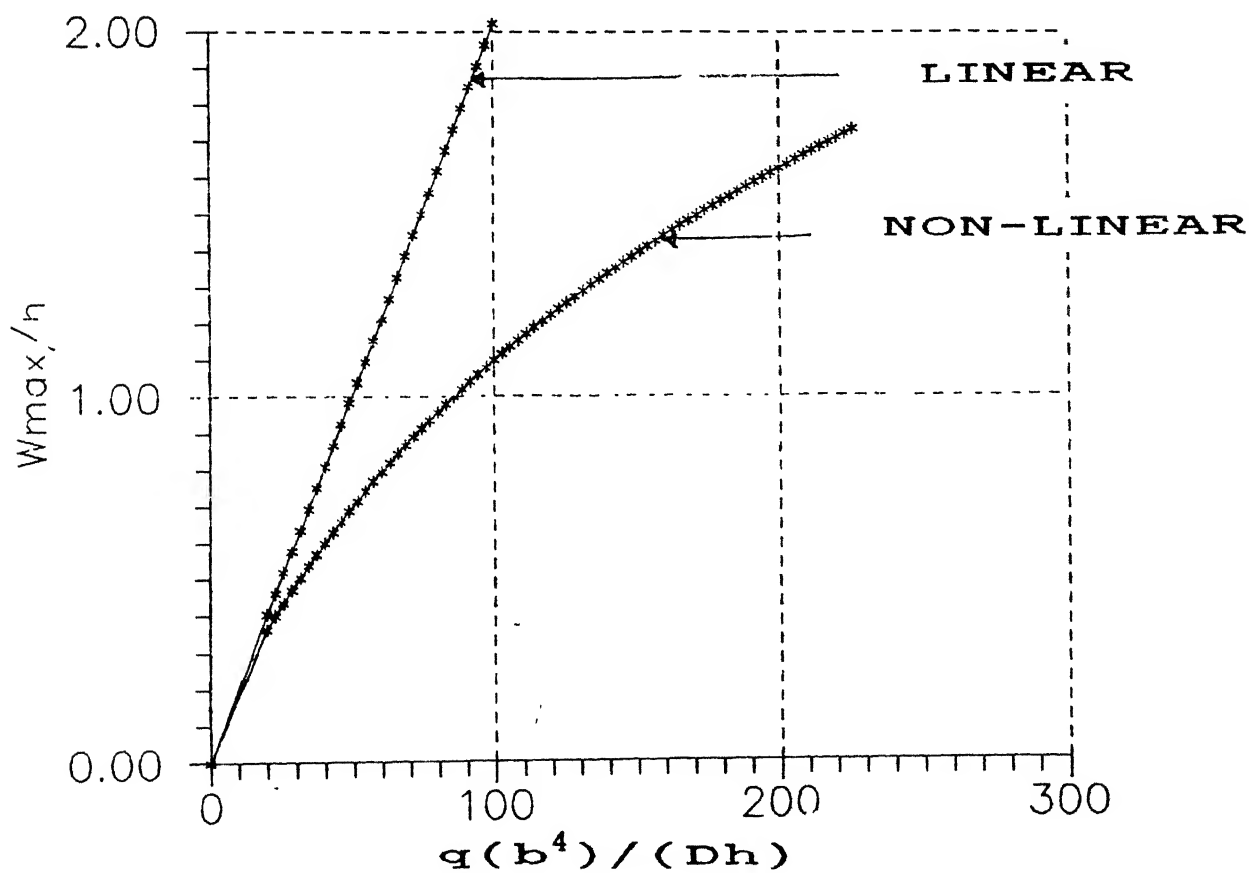


Fig 4.4(b) Results of the present method

Figure 4.4. Central deflection  $w_{max}$  of a clamped plate under uniformly distributed load.

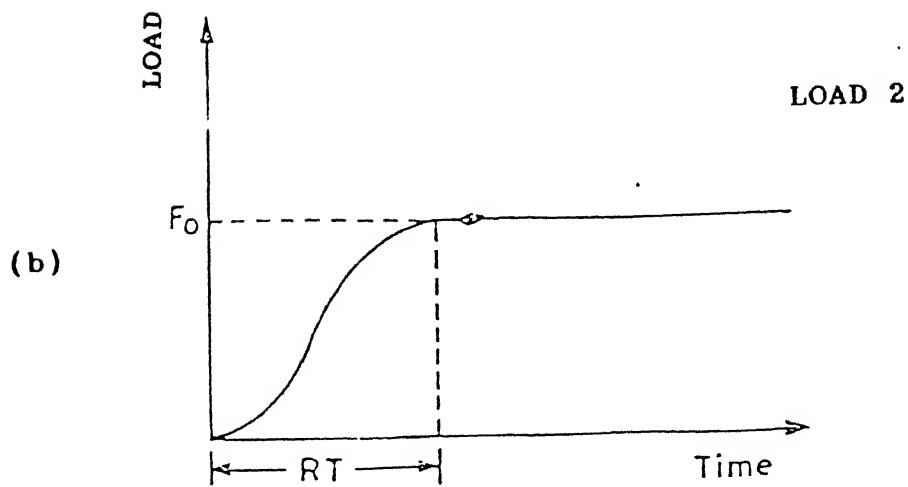
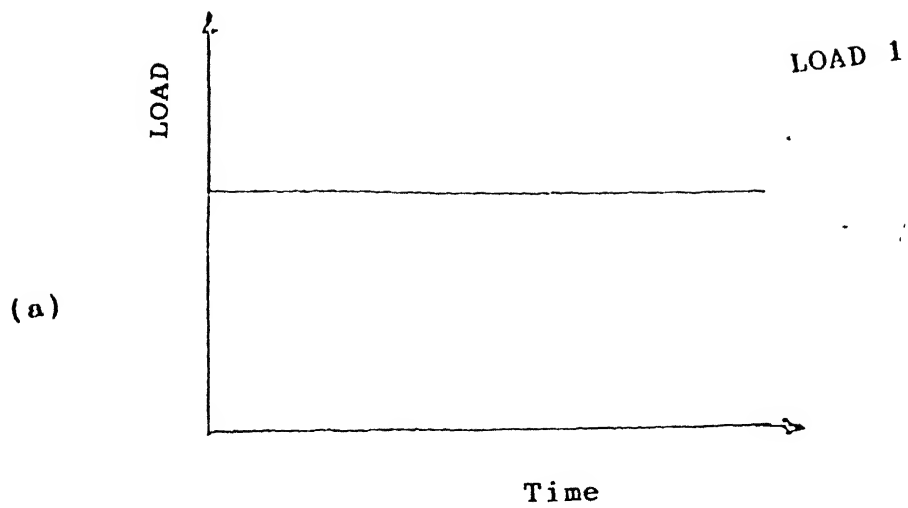


Figure 4.5. General representation of variation of force with time.

--□--□--□-- LINEAR STATIC

--○--○--○-- LINEAR DYNAMIC

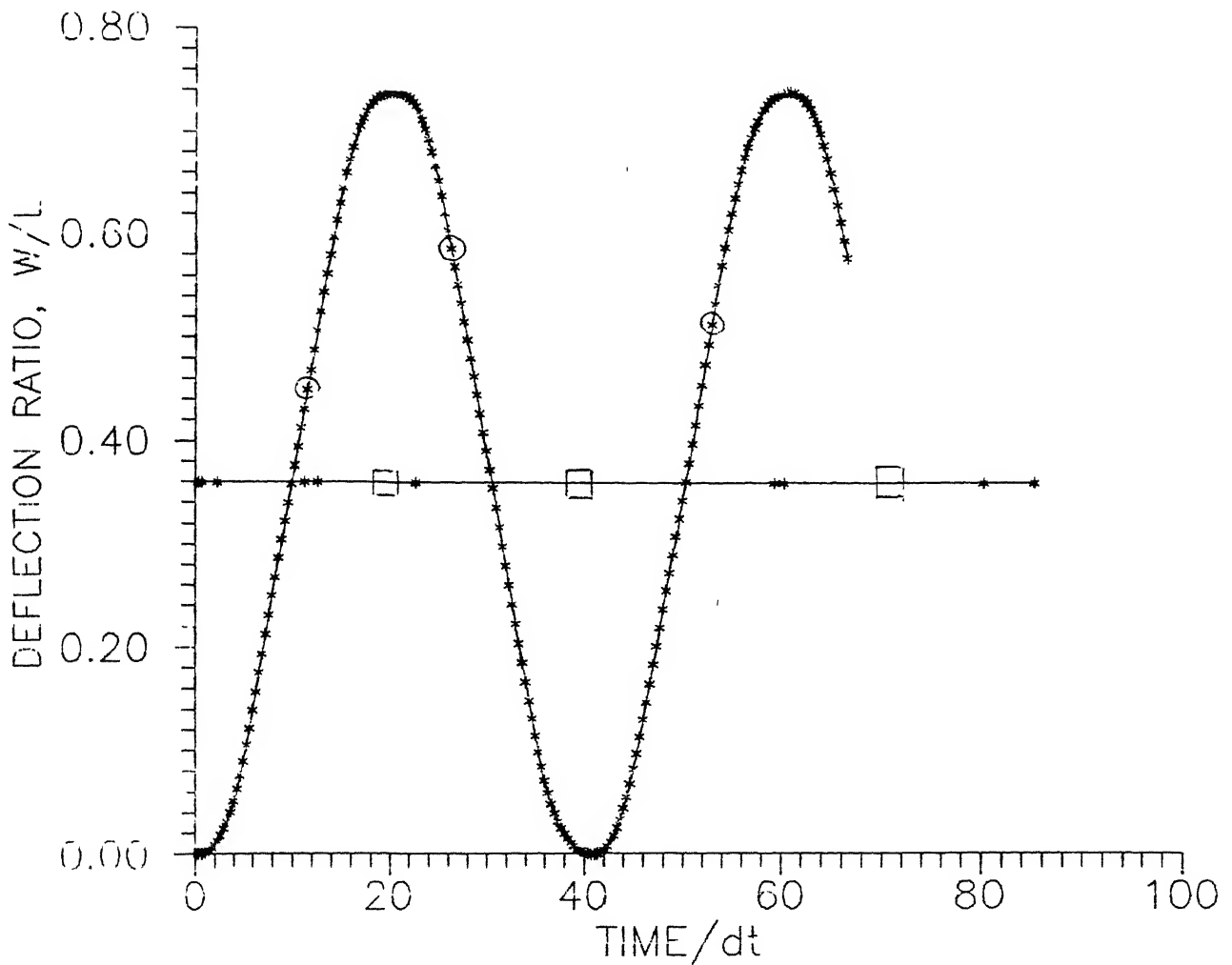


Figure 4.6. Finite displacement dynamic response of a cantilever under uniformly distributed load  $q = q_0$ , only linear case is considered.



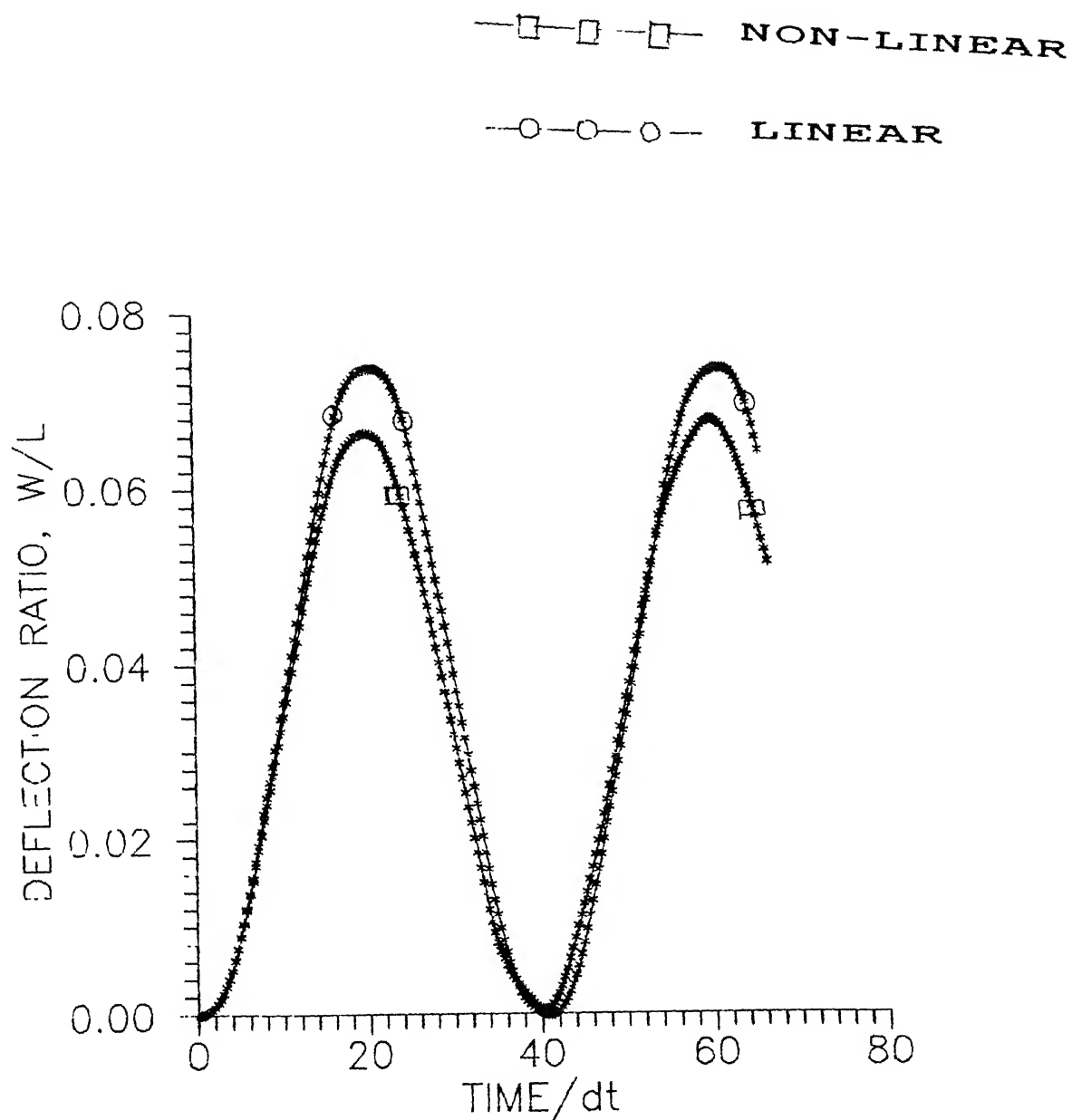


Figure 4.7a Finite displacement dynamic response of a cantilever under uniformly distributed load  $q = 0.1q_0$ , with geometric non-linearity consideration.

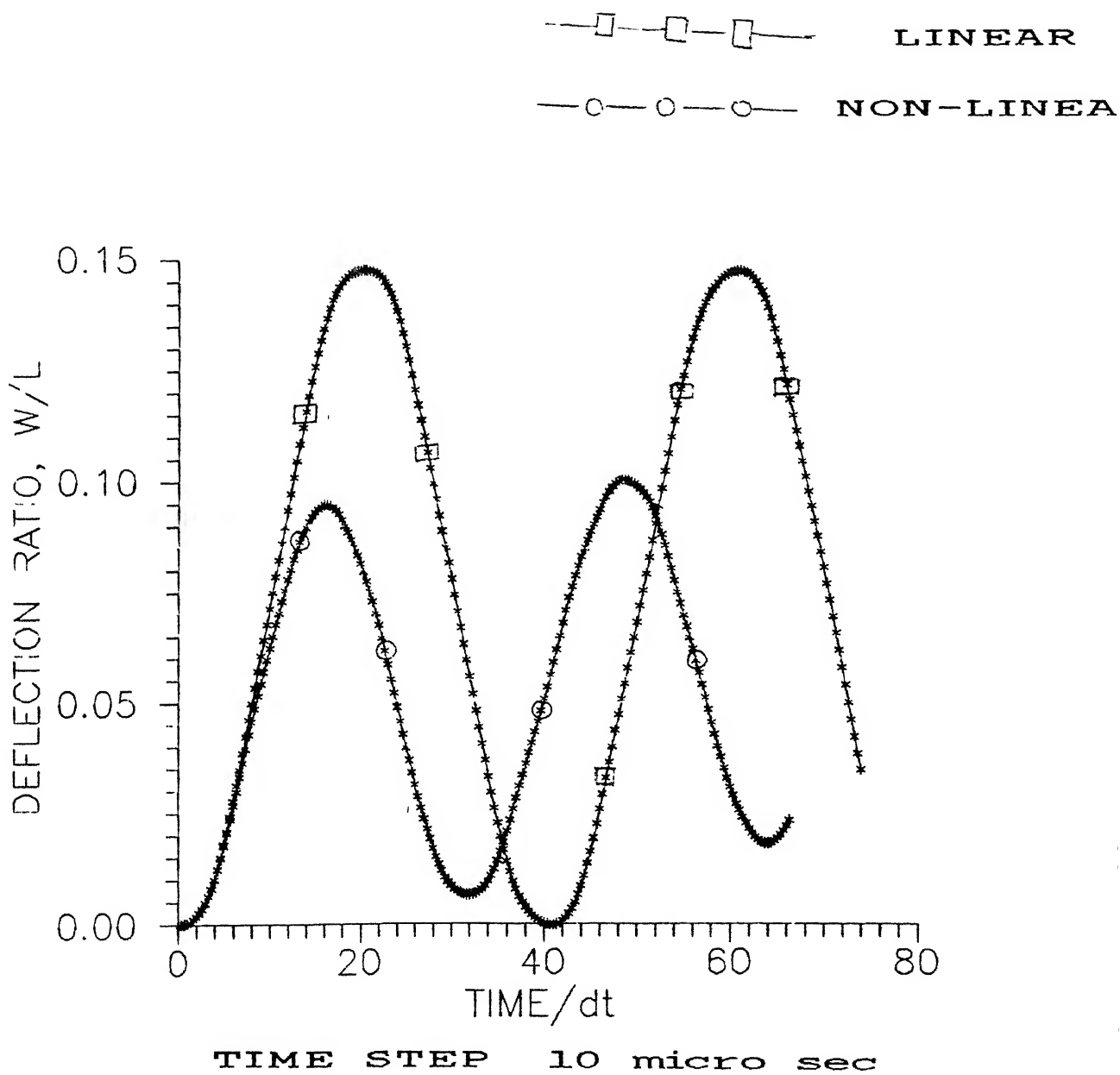


Figure 4.7b Finite displacement dynamic response of a cantilever under uniformly distributed load  $q = 0.2q_0$ , with geometric non-linearity consideration.

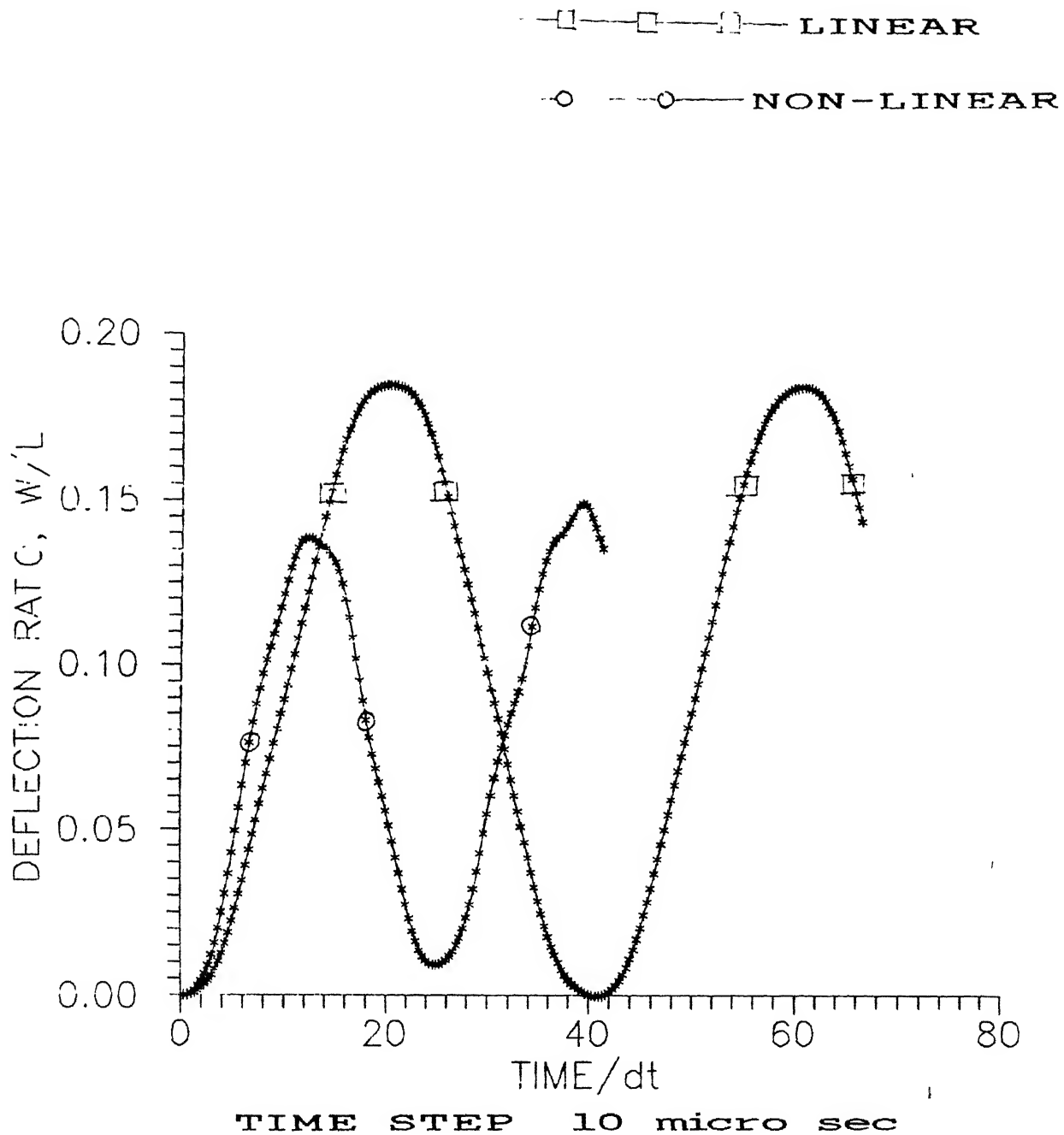


Figure 4.7c Finite displacement dynamic response of a cantilever under uniformly distributed load  $q = 0.25 q_0$ , with geometric non-linearity consideration.

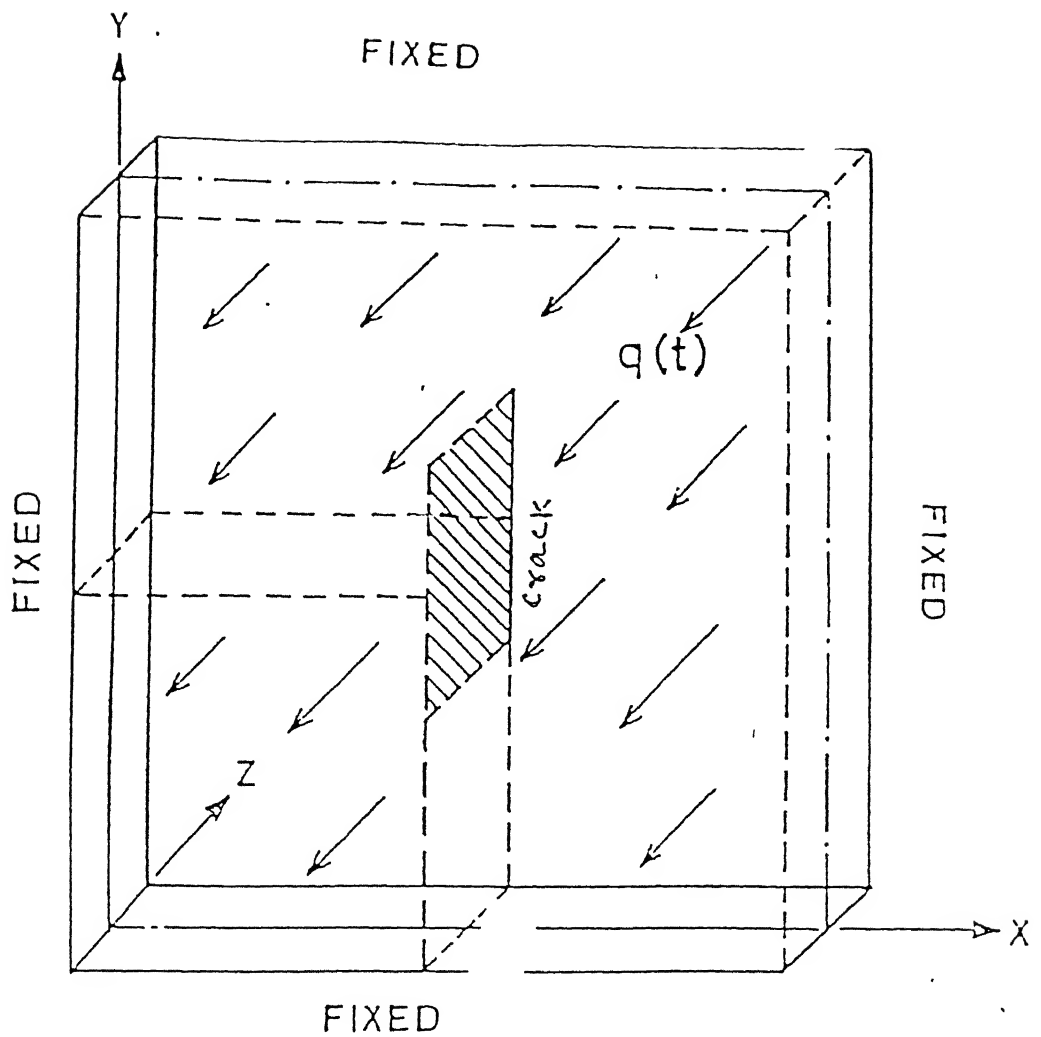


Figure 4.8 Plate with a crack under u.d.l impact fixed on all sides.

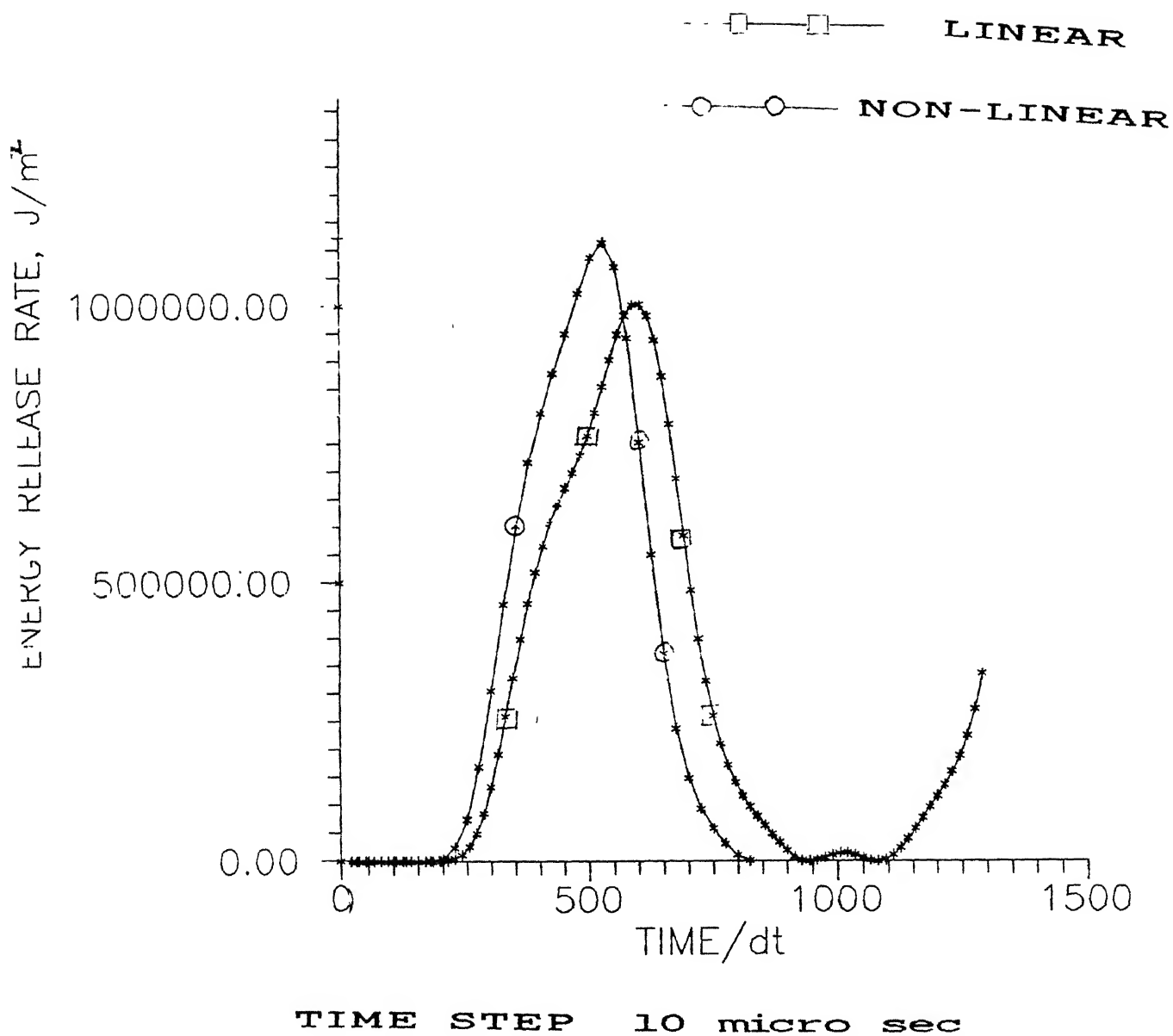


Figure 4.9 Variation of energy release rate as a function of time for a clamped plate under dynamic loading(Load #2).

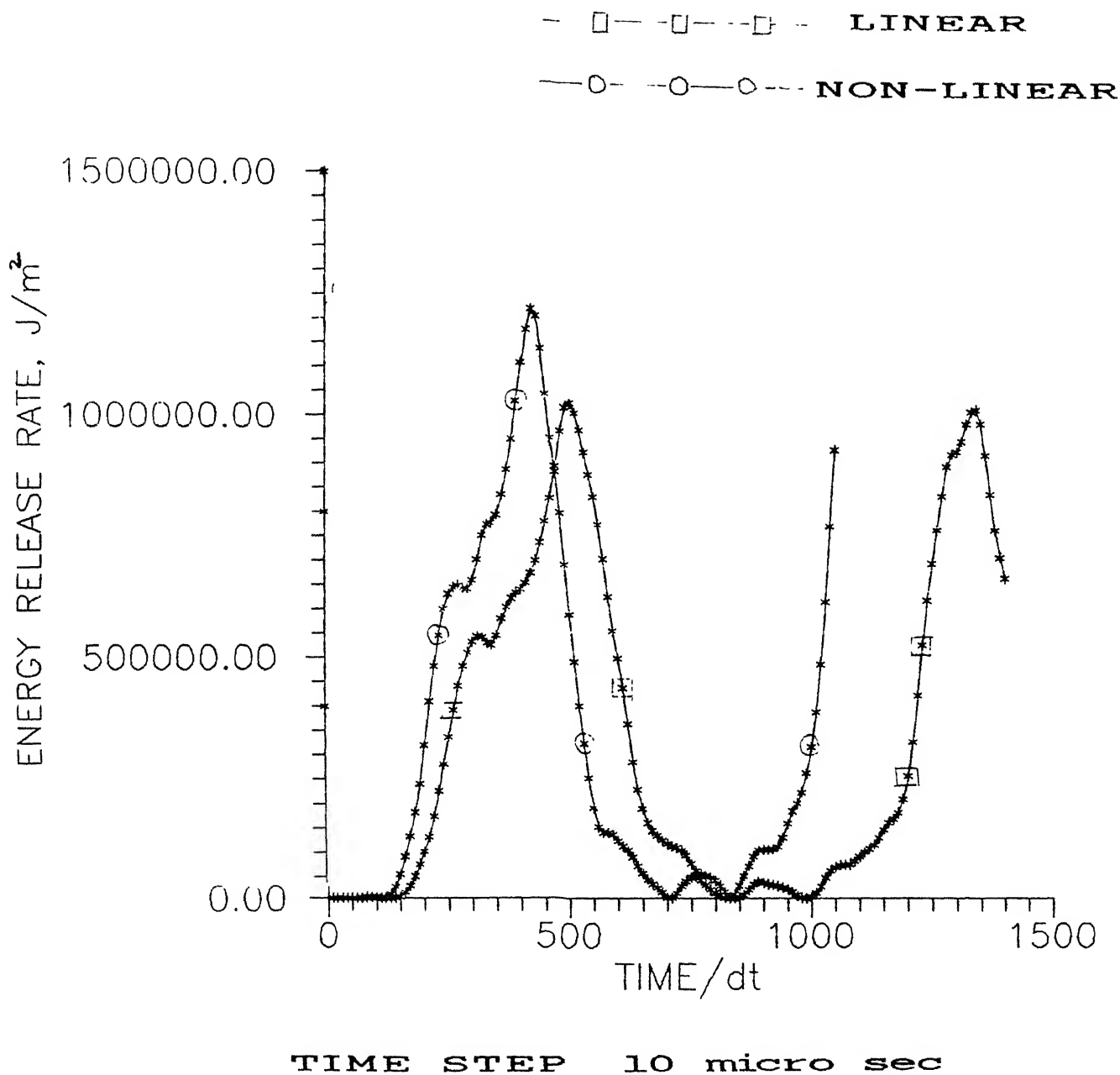


Figure 4.10 Variation of energy release rate as a function of time for a clamped plate under dynamic loading(Load #1).

## **CHAPTER 5**

### **CONCLUSIONS AND FUTURE WORK**

Based on the present finite element analysis the effect of geometric non-linearity on the behaviour of a plate with and without crack subjected to sudden loading following conclusions can be drawn:

1. Static and dynamic deflections of plate with geometric non-linearity are lower than the plate without geometric non-linearity consideration.
2. The frequency of oscillations of plate with geometric non-linearity are more than plate without geometric non-linearity consideration.
3. The effect of geometric non-linearity is highly dependent on the amount of displacements.
4. Energy release rate is 10-20 percent higher when geometric non-linearity is considered than, linear case under impact load conditions. Thus, it is important to include this effect while investigating crack initiation.

#### **SCOPE OF FUTURE WORK**

The mesh can be made finer and the time step can be made smaller to observe the sharper impact loading on plates with geometric non-linearity. It can be further modified to include large deformation and can be integrated with material non-linearity. This analysis can be tried to various configurations such as spherical shells and arches.

## REFERENCES

- Bathe, K.J., 1990, Finite Element Procedures in Engineering Analysis, Prentice Hall of India Pvt.Ltd.
- Bazant, A.P., 1978, 'Spurious reflections of elastic waves in non uniform finite element grids. ', Comp.Meth. Appl. Mech. Engg, 16, 91-100.
- Carter, L., Wellform and Halis Sen, 1981, 'A Selective Relaxation Iterative Solution Technique for Nonlinear Structural Analysis Problems', Int.. J. for Num. Methods in Engg., vol.17, 773-783.
- Dindore, U.S., 1994, 'Dynamic effect of impact load on a plate with a crack: A Finite element analysis', M.Tech. Thesis, I.I.T Kanpur.
- Dubey, R., 1993, Adaptive Finite Element Analysis of A Plate with A Crack, M.Tech Thesis, I.I.T Kanpur.
- Hinton, E. and Owen, D.R.J., 1980, Finite Element in Plasticity Theory and Practices., Pineridge Press, Swansea.
- Kishore, N. N., 'Development of Software to Analysis Cracks in a Submarine Hull', NSTL Report 1996.
- Mondkar, D.P. and Powell, G.H., 1977, 'Finite Element Analysis of Non-Linear Static and Dynamic Response', Int. J. For Num. Methods in Engg., vol. 11, pp.499-520.
- Nishioka, T., Atluri, S.N., 1986, 'Computational Methods in Dynamic Fracture', in S.N.Atluri (ed.) Computational Methods in The Mechanics of Fracture., Elsevier



Praveen Pandey., 1996, Finite Element Analysis of Elasto Plastic Dynamic Behaviour of  
Plates Under Impact Loading, M.Tech Thesis, I.I.T Kanpur.

Sih, G.C. 1977, Mechanics of Fracture, vol. 3, Plates and Shells with Cracks, Noordhoff  
Int. Publishing Leydon.

Timoshenko, S. and Woinowsky-Krieger, S., 1959, Theory of plates and shells,  
McGraw Hill Book Company Inc.

Zienkiewicz, O.C. and Taylor, R.L., 1991, The Finite Element Method, Fourth edition,  
vol.II, McGraw Hill Book Company.

Zienkiewicz, O.C. and Lefebvre, D., 1988, 'A Robust Triangular Plate Bending Element  
of The Reissner-Mindlin Type', Int. J. for Num. Methods in Engg., vol.26, 1169-1184.